DE LA RECHERCHE À L'INDUSTRIE

Theory of Neutrons and Gammas Emission in Fission

Dr. Olivier SEROT

CEA-Cadarache
DEN/DER/SPRC/LEPh
F-13108 Saint Paul lez Durance
France

www.cea.fr

Introduction

- Time scale in fission
- Energy components in fission
- Some definitions

Part I: Prompt neutron Emission

- *Mechanism of Prompt neutron emission*
- *Prompt Neutron Multiplicities*
- *Angular Distribution of Prompt neutrons*
- *Prompt Fission Neutron Spectrum (PFNS)*

Part II: Prompt gamma Emission

- *Time scale for prompt and 'late' gamma emission*
- *Available Energy for Prompt gamma Emission*
- *Prompt Fission Gamma spectrum (PFGS)*
- *Prompt Fission Gamma-ray Multiplicity*

Part III: Delayed neutron and Gamma Emission

- *Origin of the delayed neutron and gamma emission*
- *The main precursors*
- *Examples of delayed neutron and gamma spectra*
- *Influence of incident neutron energy on DN multiplicity*

Some plots shown in this document and discussions about prompt neutron and gamma emission come from lectures given by F. Gonnenwein:

F. Gonnenwein, lecture given at Ecole Joliot-Curie, 2014

F. Gonnenwein, lecture given at FIESTA-2014

Introduction

- Time scale in fission
- Energy components in fission
- Some definitions

It is important to remind the main phases occurring during the fission process, because at each phase, prompt neutrons and/or gamma may be emitted.

The prompt particle emission is governed by the available energy, the main energy components in fission will be reminded.

Lastly, some definitions will be given in this introduction.

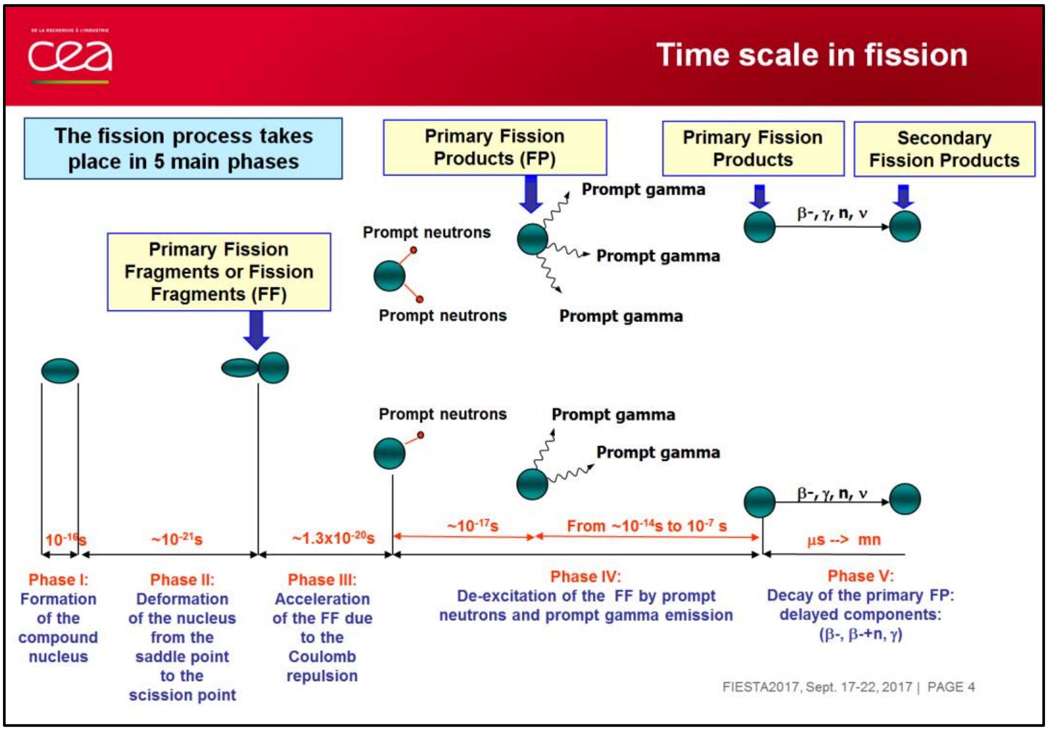

The fission process takes place into 5 main phases:

- Phase I: <u>Formation of the compound nucleus</u> (for example , in case of neutron induced fission).
- Phase II: <u>Deformation of the nucleus from the saddle point to the scission point</u>. At the scission point, primary fission fragments are assumed to be more or less deformed (compared to their ground state deformation).
- Phase III: <u>Acceleration of the FF due to the Coulomb repulsion</u>. During this phase, the nascent deformed fission fragments (at scission) will recover their ground state deformation. It means that the deformation energy at scission is transformed into intrinsic excitation energy. This phase is generally called ‘relaxation’ phase.
- Phase IV: <u>Desexcitation of the FF by prompt neutrons and prompt gamma emission</u>. Fission fragments are often highly excited and rotating. These excitation energy and spin will be dissipated by emission of prompt neutrons and/or prompt gamma particles.
- Phase V: <u>Delayed emission</u>. At this phase, the primary fission products are generally in their ground state. Since they are far from the stability valley (neutron rich nuclei), they are generally unstable (β^-). The β^- radioactivity process can be accompanied by gamma (γ), antineutrinos ($\bar{\nu}$) and sometimes by emission of one (or several neutrons). All these particles (β^-, n, γ, $\bar{\nu}$) are called ‘delayed particles’, because they are emitted several order of magnitude in time after the beginning of the fission process.

Note: Prompt particle emission occurs mainly during the phase IV. Nevertheless, as we will see later, additional prompt neutrons may be emitted during the three first phases.

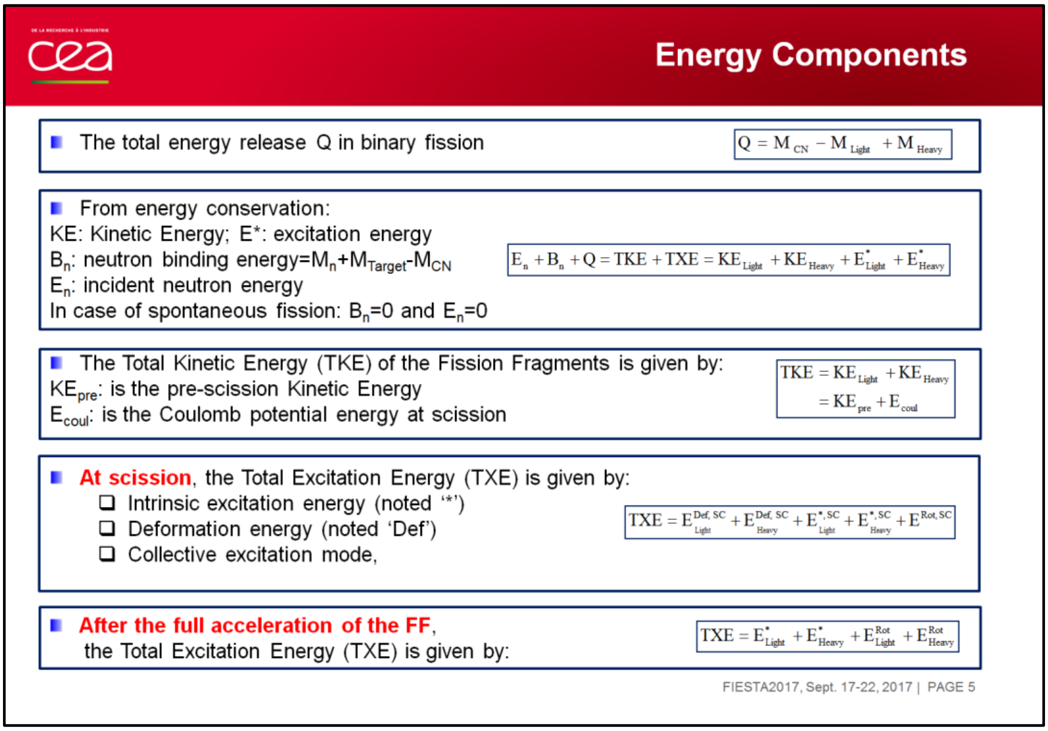

- The total energy release Q in binary fission is defined as the ground-state mass of the compound nucleus fissioning nucleus minus the ground-state masses of the two binary fission fragments.
- From energy conservation: En+Bn+Q is equal to the total kinetic energy (TKE) and the total excitation energy (TXE) of the fission fragments.
- TKE is the sum of two terms: KEpre, which corresponds to the pre-scission kinetic energy (not well known) and Ecoul, which corresponds to the Coulomb energy. Ecoul can be accurately calculated only if the deformation of the two nascent fission fragments (at scission) is known (which is not the case !).
- The total excitation energy at scission has three components: (1) Intrinsic excitation energy (noted with '*') which correspond to the excitation of individual nucleons; (2) Deformation energy (noted 'Def') which corresponds to the deformation energy of the nucleus at the scission point compared to its ground state deformation; (3) Collective excitation energy, which corresponds in first approximation to rotational energy. Again, these three components are poorly known.
- After the full acceleration of the FF, their deformation energy is assumed to be transformed into intrinsic excitation energy ('relaxation' phase). In addition, due to their spin, these FF have a collective rotational energy. So, after the relaxation phase TXE has only two components (intrinsic and rotational). The calculation of the rotational energy requires the knowledge of the fission fragment J, which is unfortunately poorly known. In additional, the partitioning of the intrinsic excitation energy between the two fragments remains an open question.

A nice discussion on the energy balance involved in fission is given in:

H. Marten and A. Ruben, Sov. At. Ener. 69, 583 (1990)

A. Ruben and H. Marten and D. Seeliger, Z. Phys. A, Hadrons and Nuclei, 338, 67-74 (1991)

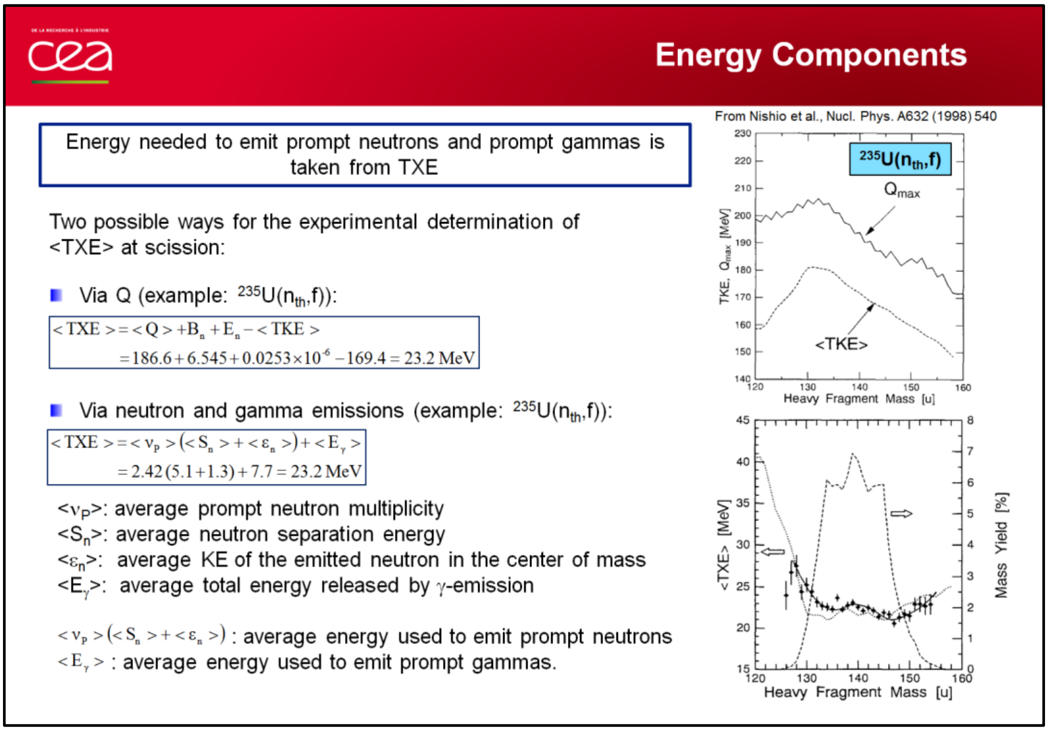

TXE is of particular importance, because it corresponds to the energy used to emit prompt neutrons and prompt gammas.

The two procedures to get the average excitation energy available at scission are very consistent each others.

The experimental data mentioned on this slide are taken from: Nishio et al., Nucl. Phys. A632 (1998) 540

Energy Components

Excitation Energy

Average Total Excitation Energy <TXE>

for thermal neutron induced fission reactions and spontaneous fission of actinides (From Gonnenwein, lecture Ecole Joliot-Curie, 2014)

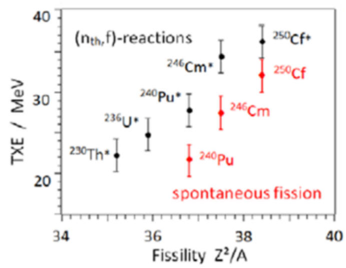

Average excitation energy <E*> as a function of mass

Pre-neutron mass yield plotted on the right scale (red curve).

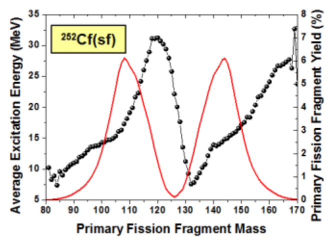

Kinetic Energy

Average Total Kinetic Energy <TKE>

(from Zhoa et al. PRC 62, 014612 (2000))

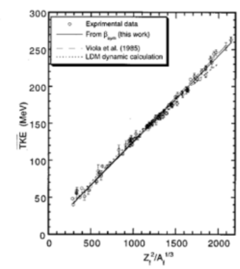

Average kinetic energy <KE> as a function of mass

Pre-neutron mass yield plotted on the right scale (red curve).

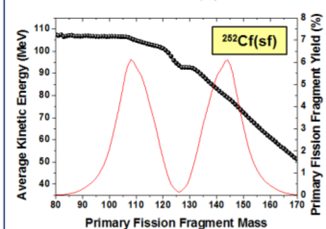

Some definitions

Following the discussion proposed by D. Madland, 2006

- ❑ Primary fission fragment
- ❑ Secondary fission fragment
- ❑ Fission products

- ❑ Prompt neutrons
- ❑ Prompts gamma
- ❑ Late gamma
- ❑ Delayed neutrons
- ❑ Delayed Gamma

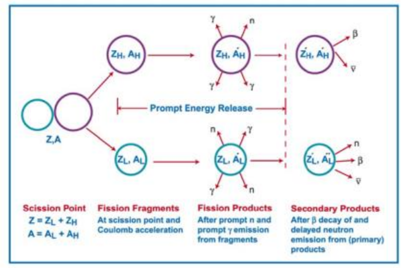

- ***Primary Fission fragment*** *(or Fission Fragment)*: Nuclear species existing at the scission point and just beyond, but prior to the emission of prompt neutrons and prompt gamma rays.
- ***Primary Fission product*** (or *Fission product*): Nuclear species existing following prompt neutron emission and prompt gamma emission from a fragment, but before any β decay has occurred.
- ***Secondary fission product***: Nuclear species existing following at least one β decay of a primary fission product.

FIESTA2017, Sept. 17-22, 2017 | PAGE 8

These definitions are given in the Madland ‘s paper:

D.G. Madland, Nucl. Phys. A772, 113 (2006)

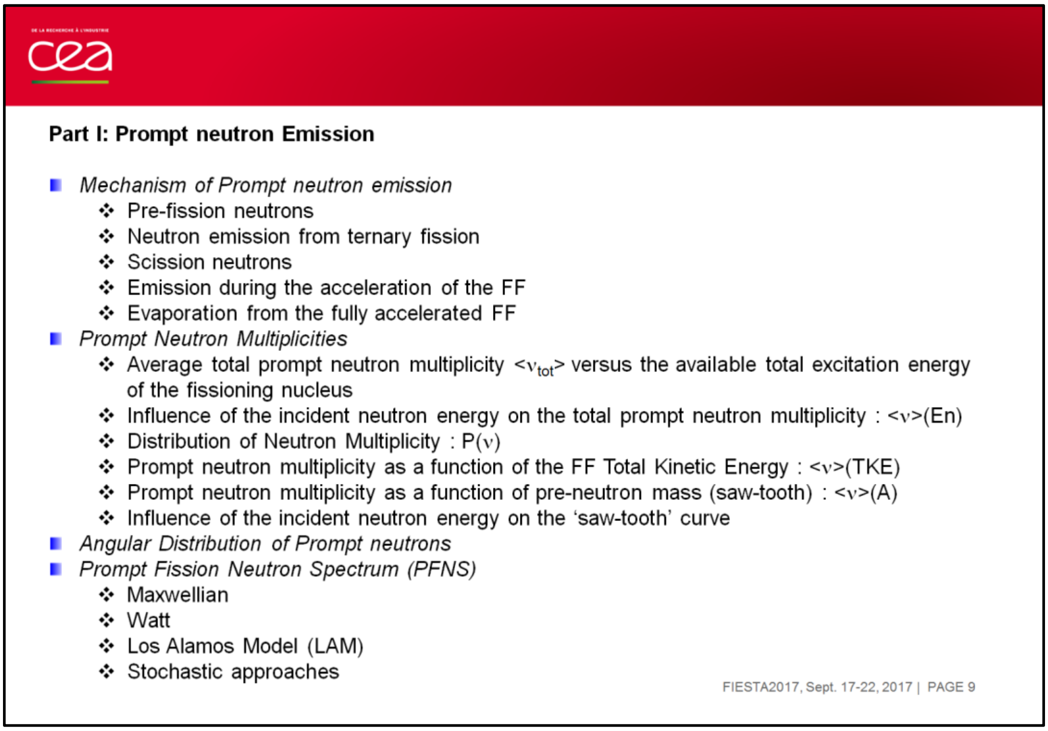

Part I of this lecture is related to the prompt neutron emission.

Mechanisms of prompt neutron emission are first described.

Prompt neutron multiplicities will be then discussed. Some correlations between multiplicity and other fission observables are shown. These correlations are very useful to improve our knowledge of the fission process.

The angular distribution of the prompt neutron with FF is also a nice tool to investigate the emission process.

Lastly, several models used to describe Prompt Fission Neutron Spectra (PFNS) will be presented.

Part I: Prompt neutron Emission

- *Mechanism of Prompt neutron emission*
  - Pre-fission neutrons
  - Neutron emission from ternary fission
  - Scission neutrons
  - Emission during the acceleration of the FF
  - Evaporation from the fully accelerated FF

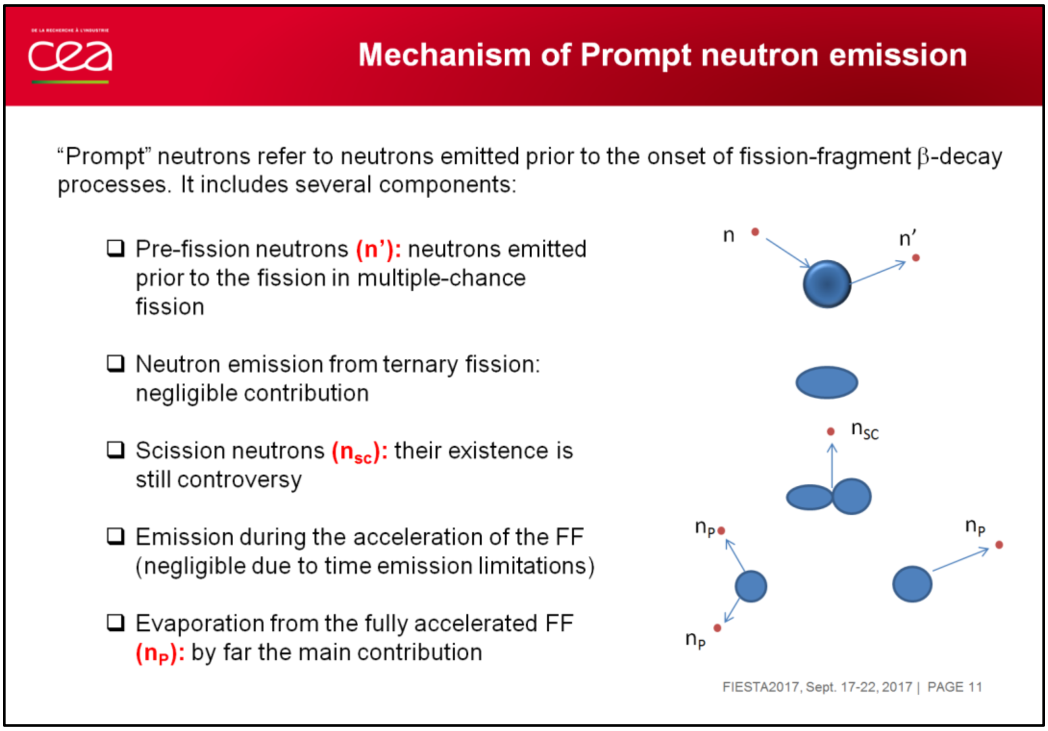

As already mentioned, even if neutrons evaporated from the fully accelerated FF is by far the main prompt neutron component, other possible source of neutrons exist.

In principle, for the applications in nuclear energy, if we want to be able to describe the total prompt fission neutron spectrum or the total prompt neutron multiplicity, all these additional sources must be accounted for.

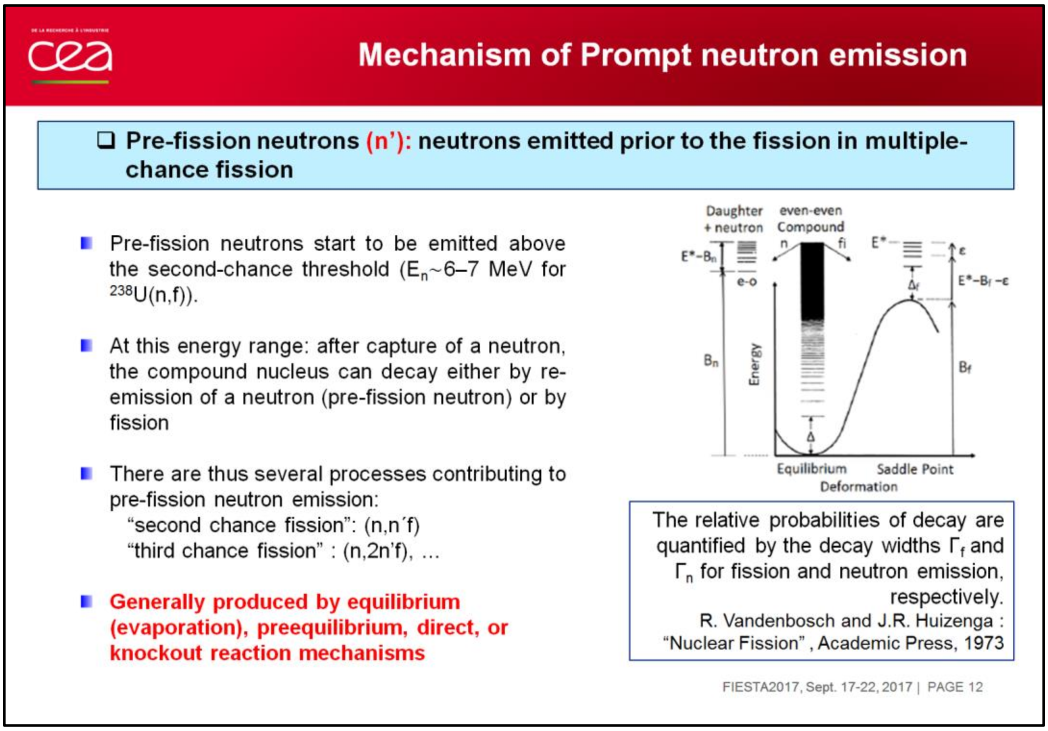

Pre-fission neutrons start to be emitted above the second-chance threshold (E_n~6–7 MeV for ^{238}U(n,f)). At this energy range, after capture of a neutron, the compound nucleus can decay either by re-emission of a neutron (pre-fission neutron) or by fission. Below this second-chance threshold, the excitation energy of the residual nucleus left after neutron emission is too low to undergo fission (neglecting tunneling through the barrier). The plot below gives an example of the several fission chances occurring in the neutron-induced fission of ^{235}U (from JEFF-3.1 library)

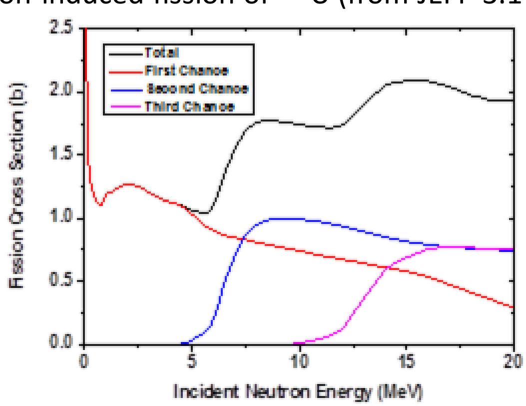

These pre-fission neutrons have therefore nothing to do with the fission process. Their emission comes from an evaporation process (equilibrium), or preequilibrium, or direct reaction, or knockout reaction, depending on the incident neutron energy.

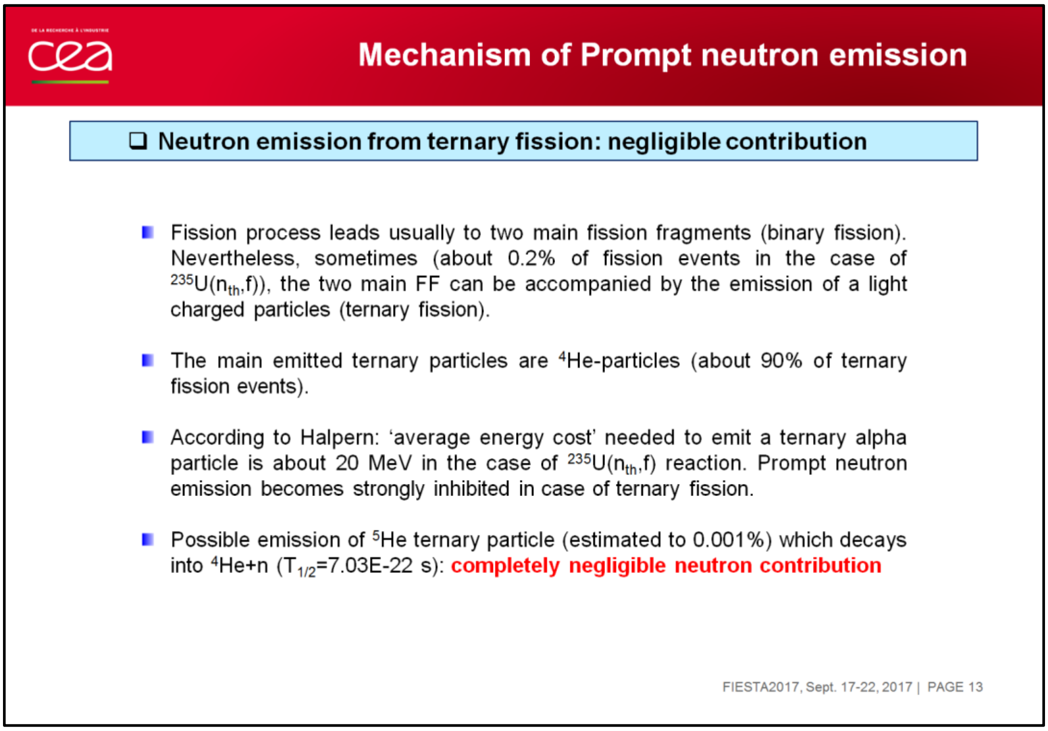

Fission process leads usually to two main fission fragments (binary fission). Nevertheless, sometimes, the two main FF can be accompanied by the emission of a light charged particles (ternary fission). This phenomenon is rare: about 0.2% of fission events in the case of $^{235}U(n_{th},f)$. The main emitted ternary particles are ^{4}He-particles (about 90% of ternary fission events).

In case of ternary fission event, the two main fragments have less available excitation energy, because part of this energy is taken to emit the ternary particle. For example, according to Halpern, the ‘average energy cost’ needed to emit a ternary alpha particle is about 20 MeV in the case of $^{235}U(n_{th},f)$ reaction. Keeping in mind that the total average excitation energy is about 24 MeV for this reaction, we see that prompt neutron emission becomes strongly inhibited in case of ternary fission.

It is also interesting to mention that ternary ^{5}He particles can be emitted (about 0.001% of fission events). Due to its very short half life ($T_{1/2}$=7.03E-22 s), ^{5}He ternary particles decay by emitting a neutron: $^{5}He \rightarrow {}^{4}He+n$

The multiplicity of these neutrons originating from the decay of ^{5}He is obviously completely negligible.

Mechanism of Prompt neutron emission

❑ **Scission neutrons (n_{sc}): their existence is still controversy**

- **Poor and contradictory experimental data:** difficulty to distinguish experimentally neutrons from fully accelerated FF (evaporated neutrons) and neutrons emitted at the scission point (scission neutrons).

Author	Contribution	
Franklyn, 1978	20%	$^{235}U(n_{th},f)$
Vorobyev, 2009	5%	$^{235}U(n_{th},f)$
Bowman, 1962	10%	$^{252}Cf(sf)$
Marten, 1989	<1%	$^{252}Cf(sf)$
Budtz-Jorgensen, 1989	<1%	$^{252}Cf(sf)$
Kornilov, 2001	10%	$^{252}Cf(sf)$
Gagarski, 2012	8%	$^{252}Cf(sf)$
Chietera, 2014	8%	$^{252}Cf(sf)$

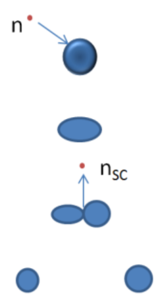

- **Argument in favor of scission neutrons:**
  - ❑ Ternary light charged particles can be emitted at the scission point. 'Ternary neutrons' (or scission neutrons) should therefore also exist
  - ❑ Could be even the most produced ternary particles because no Coulomb barrier has to be overcame for their emission (require less energy to be emitted)

The existence of scission neutrons (neutron emitted close in time to the scission point) is still an open question. It is mainly due to the poor and contradictory experimental data (see the table, where scission neutron contributions compared to the total prompt neutron multiplicity are given). Experimentally, the capability to distinguish neutrons emitted from the fully accelerated FF (evaporated neutrons) and neutrons emitted at the scission point (scission neutrons) is not straightforward.

Nevertheless, there are various strong arguments in favor of the existence of scission neutrons. In particular, we know that various ternary light charged particles can be emitted at the scission point: ^{1}H, ^{2}H, ^{3}H, ^{4}He,. . . up to A=40. 'Ternary neutrons' (or scission neutrons) should therefore also exist and could be even the most produced ternary particle because no Coulomb barrier has to be overcame for their emission, meaning that scission neutrons require less energy to be emitted than the other ternary charged particles.

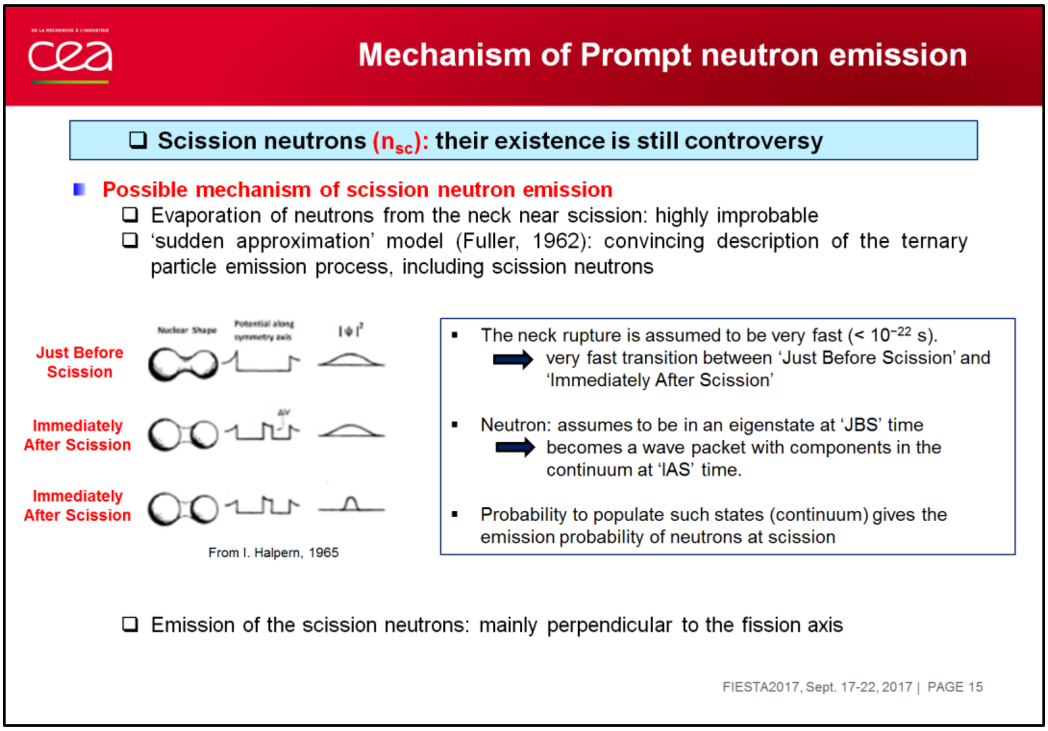

A possible mechanism of the scission neutron emission is discussed in this slide.

- Evaporation of neutrons from the neck near scission is highly improbable, since the typical time of evaporation ($\sim 10^{-18}$ s) is longer than the time involved in the descent from saddle to scission ($< 10^{-20}$ s).
- The so-called 'sudden approximation' model proposed initially by Fuller is a convincing description of the ternary particle emission process, including scission neutrons.

In this model, the neck rupture is assumed to be very fast ($< 10^{-22}$ s). In other words, the transition from two fragments connected by a thin neck to two separated fragments happens in a very short time (see the figure from Halpern).

Due to this assumed loss of adiabaticity during the neck rupture, the eigenstate describing a neutron 'Just before scission' is defined at the 'Immediately After Scission' (IAS) time by the same wave function, which is now a wave packet (in the new IAS potential), with components in the continuum energy region.

The probability to populate the continuum states corresponds to the neutron emission probability at scission. This probability is not easy to calculate because it depends strongly on the 'Just Before Scission' and 'Immediately after scission' configurations chosen.

Whatever those configurations, the emission of the scission neutrons takes place mainly perpendicularly to the fission axis leading to a strong anisotropy.

Mechanism of Prompt neutron emission

❑ Emission during the acceleration of the FF

Part of the prompt neutrons can be emitted during the acceleration phase of the primary fission fragments ? To answer, we need to know:

t Characteristic time of the acceleration phase (Coulomb repulsion)
τ Characteristic time associated to neutron evaporation.

- **Estimation of *t***

$$\frac{\mu}{0.5}\left(\frac{dr}{dt}\right)^2 + \frac{Z_L Z_H e^2}{r} = E_{Coul} + E_{pre}$$

μ: reduced mass of the two FF
r: distance between the two charge centers
Z_L, Z_H: nuclear charges
E_{pre}: pre-Kinetic energy
E_{Coul}: Coulomb repulsion
when: $r \rightarrow \infty$, $E_{Coul}+E_{pre}$=TKE

Example: adopting E_{pre}=0,
90% of the TKE is reached after **8.6×10^{-21} s**

From 'The fission process', CRP press, 1993

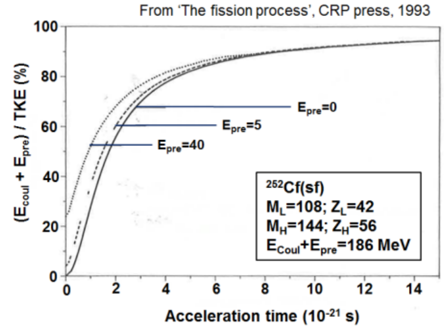

As already mentioned, the pre-scission kinetic energy (KEpre) is a poorly known quantity. Several arbitrary KEpre values have been chosen to perform the calculations. It doesn't impact the time needed by the FF to reach 90% of the total kinetic energy.

Figure from:

H.-H. Knitter, et al., in "The Nuclear Fission Process", C. Wagemans ed., CRC Press 1991

Mechanism of Prompt neutron emission

❑ Emission during the acceleration of the FF

Estimation of τ

According to Ericson, the probability to decay by neutron emission is a time-dependent function given by:

$$\boxed{P(t) = 1 - P_0 \exp(-t/\tau)}$$

Where the decay time τ is obtained from:

$$\boxed{\tau(s) = 1\times10^{-21} \frac{2A^{1/3}}{(E^*-S_n)} \exp\left(\frac{S_n}{T}\right)}$$

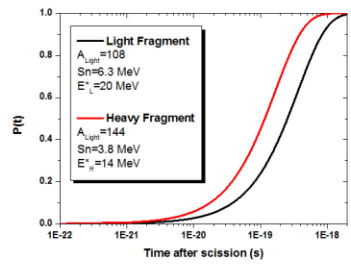

These probabilities are plotted for typical Light and Heavy Fragment pair appearing during the spontaneous fission of ^{252}Cf:

$$\boxed{\begin{aligned}\tau_{Light} &= 3.7\times10^{-19}\,s \\ \tau_{Heavy} &= 1.7\times10^{-19}\,s\end{aligned}}$$

Conclusion

Since the decay time associated to the neutron emission seems to be longer than the acceleration phase time ($\tau > t$): **neutron emission during this phase is probably negligible**.

FIESTA2017, Sept. 17-22, 2017 | PAGE 17

Note that the typical time of evaporation obtained from Ericson's equation is close to the one obtained from the neutron widths. Indeed, the neutron width of states of the primary FF with an excitation energy above Sn and 30 MeV fluctuates around several tens of eV. From the Heisenberg's uncertainty relation, we have:

$\tau=\hbar/\Gamma n$. With Γn=100eV, we get $\tau=6\times10^{-18}$s

References:

T. Ericson and V. Strutinski, Nucl. Phys. 8, 284 (1958)

T. Ericson, Advances in Nuclear Physics **6**, 425 (1960)

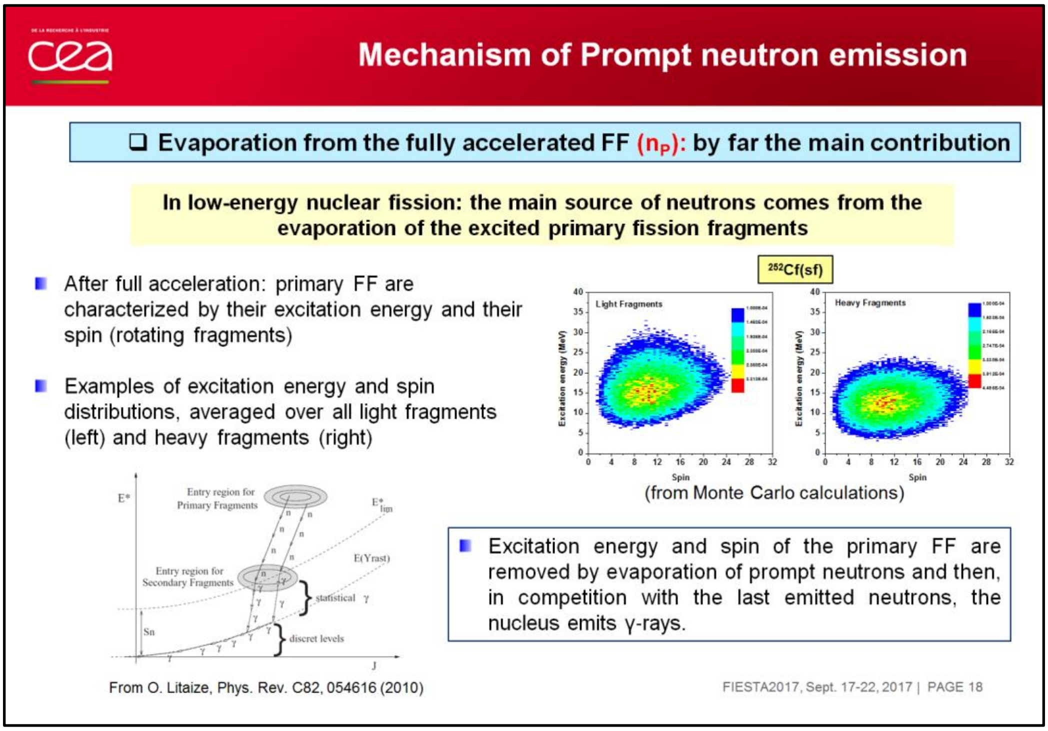

The excitation energy and spin distributions for the light and heavy fragments shown here come from Monte Carlo simulation for 252Cf(sf). From this calculation, we can see that the light fragment group has, in average, more excitation energy available (<E*_Light>=19.8 MeV) than the heavy fragment group (<E*_Light>=14.4 MeV).

Part I: Prompt neutron Emission

- *Prompt Neutron Multiplicities*
  - Average total prompt neutron multiplicity $<\nu_{tot}>$ versus the available total excitation energy of the fissioning nucleus
  - Influence of the incident neutron energy on the total prompt neutron multiplicity : $<\nu>(En)$
  - Distribution of Neutron Multiplicity : $P(\nu)$
  - Prompt neutron multiplicity as a function of the FF Total Kinetic Energy : $<\nu>(TKE)$
  - Prompt neutron multiplicity as a function of pre-neutron mass (saw-tooth) : $<\nu>(A)$
  - Influence of the incident neutron energy on the 'saw-tooth' curve

Prompt Neutron Multiplicities

❑ Average total prompt neutron multiplicity $<\nu_{tot}>$ versus the available total excitation energy of the fissioning nucleus

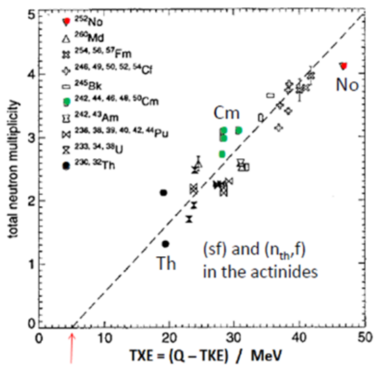

From F. Gonnenwein, lecture FIESTA-2014, extracted from D. Hilscher and H. Rossner: Ann. Phys.(Paris), 17 (1992) 471

- As expected: a clear increase of $<\nu_{tot}>$ observed with increasing <TXE>

In the figure: <TXE> calculated from:
$<TXE> = <Q> + B_n + E_n - <TKE>$
(B_n and E_n are zero in case of spontaneous fission).

- Offset observed at about 5 MeV (red arrow): when <TXE> is lower than the neutron binding energy, prompt neutron emission becomes energetically not possible. Only prompt gamma rays will be emitted to cold the nucleus.

- Slope of the linear fit : 0.112 n/MeV

Prompt Neutron Multiplicities

❑ Influence of the incident neutron energy on the total prompt neutron multiplicity : <ν>(En)

- Increase of the prompt neutron multiplicity with incident neutron energy: ^{239}Pu(n,f) (top) and ^{235}U(n,f) (bottom)
- When 2nd and higher chance fissions are setting in (En higher than about 5 MeV for ^{235}U(n,f)), two components:
  - ❑ **Component 1** (red curve): neutrons evaporated by the fragments
  - ❑ **Component 2** (blue curve): neutrons re-emitted by the compound nucleus before fission ("pre-scission neutrons")
- Note: After first fission chance, 'evaporated' neutron multiplicity component is decreasing around 6 MeV (red curve) : after emission of a pre-fission neutron, the residual compound nucleus (A-1) has less available excitation energy.

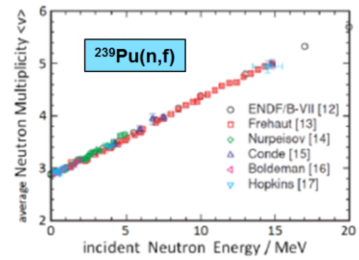

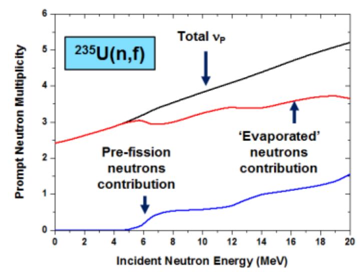

Prompt Neutron Multiplicities

❑ Distribution of Neutron Multiplicity : P(ν)

- Examples of measured P(ν) (normalized to one) for three fissioning systems
- P(ν) well reproduced by a Gaussian curve characterized by:
  - ❑ The average value: <ν>
  - ❑ The variance: σ^2
- For actinides (from Pu to Cm): variances rather constant, For Cf to No: variances rise significantly.

Nucleus	238U	238Pu	240Pu	242Pu	242Cm	244Cm	246Cm	248Cm	246Cf	250Cf	252Cf	254Cf	256Fm	257Fm	252No
σ^2	0.902	1.278	1.303	1.340	1.220	1.263	1.285	1.304	1.680	1.534	1.596	1.529	2.219	2.493	4.284

Variance data from spontaneous fissioning systems

- P(ν=0): neutron-less fission (also called 'cold fission'). May be very different from one fissioning nucleus to another. Examples $^{235}U(n_{th},f)$ (<ν> = 2.42) ➡ P(ν=0)=3.2%
  $^{252}Cf(sf)$ (<ν> = 3.76) ➡ P(ν=0)= 0.23%

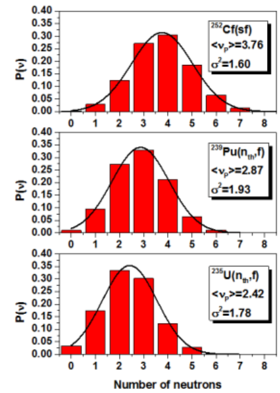

Measured distribution of the neutron multiplicity P(ν) for 3 fissioning nuclei: ^{252}Cf(sf) (from Vorobyev, 2004); $^{235}U(n_{th},f)$ (from J.W. Boldeman ,1985); $^{239}Pu(nt_{h},f)$ (from Gwin, 1984)

Experimental data come from the following references:

A.S. Vorobyev *et al.*, Proc. Int. Conf. Nuclear Data Science Technology, Santa Fe, USA, 2004, AIP Proceedings CP769, 613 (2005)

J.W. Boldeman and M. G. Hines, Nucl. Science and Eng. 91 (1985) 114

R. Gwin, Nucl. Sci. Eng 87,381 (1984)

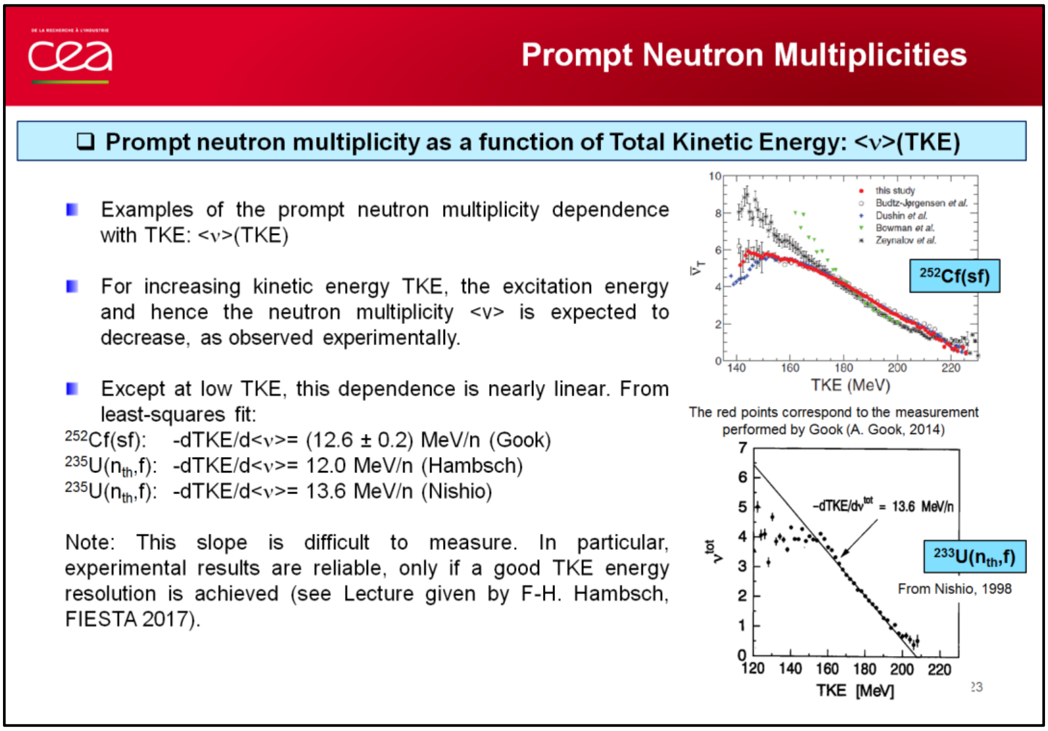

Experimental data come from the following references:

A. Gook, et al., Phys. Rev. C 90, 064611 (2014)

K. Nishio, et al., Nucl. Phys. A 632, 540 (1998).

K. Nishio, et al., Journal of Nuclear Science and Technology, 35, 631 (1998)

Sh. Zeynalov et al., J. Korean Phys. Soc. **59**, 1396 (2011)

C. Budtz-Jørgensen and H.H. Knitter, Nucl. Phys. A 490, 307 (1988)

Prompt Neutron Multiplicities

❑ Prompt neutron multiplicity as a function of pre-neutron mass: <ν>(A)

- Plotted as a function of primary fragment mass, the average multiplicity <ν>(A) has a saw-tooth like appearance.
- Observed for all fissioning systems, but more pronounced at low fission energy
- In heavy mass region: a clear minimum is observed around the mass 130
- On average, light fragment group emits generally more neutrons than the heavy fragment group (at least for thermal neutron-induced fission and spontaneous fission): $\boxed{<\nu_{Light}> \geq <\nu_{Heavy}>}$

$$<\nu_{Light}> = \sum_{A_{pre} \in Light} Y(A_{pre}) <\nu_{Light}>(A_{pre})$$
$$<\nu_{Heavy}> = \sum_{A_{pre} \in Heavy} Y(A_{pre}) <\nu_{Heavy}>(A_{pre})$$

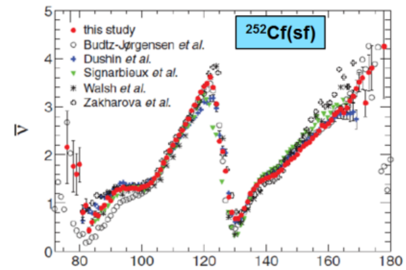

The red points correspond to the measurement performed by Gook (A. Gook, 2014)

Some examples

Reaction	$^{233}U(n_{th},f)$	$^{235}U(n_{th},f)$	$^{252}Cf(sf)$
ν_L / ν_H	1.395/1.100	1.390/1.047	2.056/1.710
Ratio	1.27	1.33	1.20

FIESTA2017, Sept. 17-22, 2017 | PAGE 24

The average prompt neutron for the light and heavy fragments can be obtained from the 'saw-tooth' curve by weighing it with the pre-neutron mass yield (see equations at the bottom of the slide).

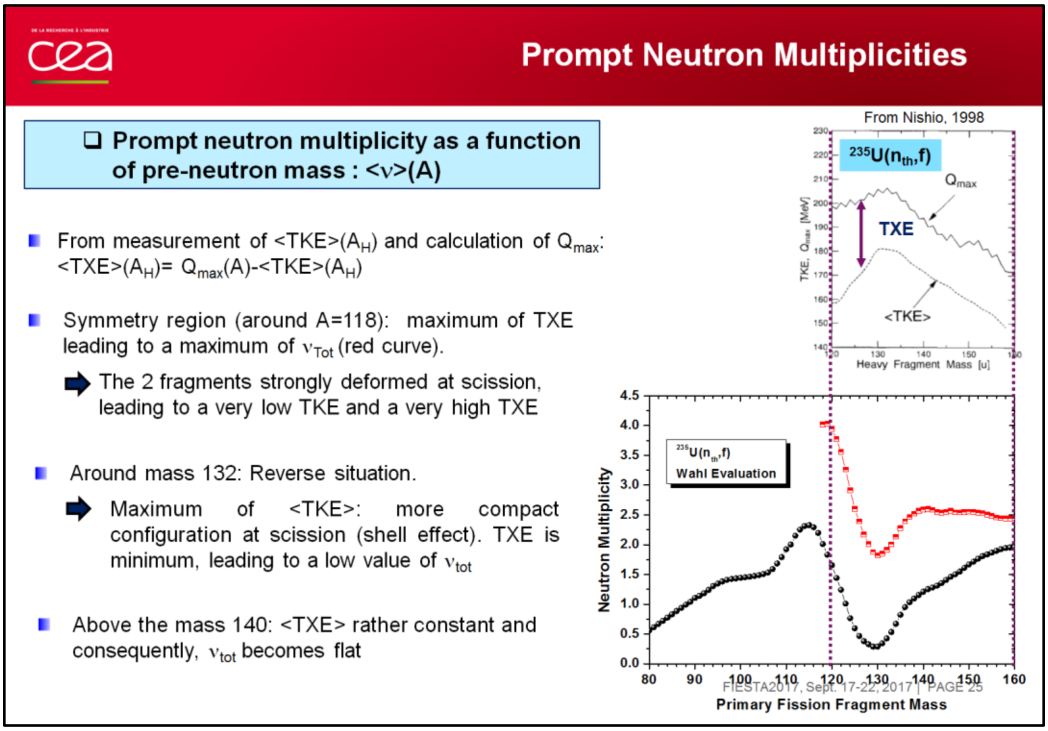

- From the measurement of <TKE>(A_{pre}) and the calculation of Q_{max} (here, the maximum Q-value, Q_{max}, is set to the highest Q-value in the three charge-splits around the most probable charge division), it is possible to estimate <TXE>(A_{pre}) (see top of the figure): <TXE>(A_{pre})= Q_{max}(A)-<TKE>(A_{pre})
- Near the symmetry (A=118, for ^{235}U(n_{th},f) reaction), a maximum of TXE occurs, which consequently leads to a maximum in the total prompt neutron multiplicity (red curve). It suggests that in the symmetry region, the two nascent fragments are strongly deformed at scission leading to a very low TKE and therefore a very high TXE.
- At around mass 132, the reverse situation occurs: we observe a maximum of <TKE>, which is the signature of a more compact configuration at scission. It is due to the double magic nucleus (^{132}Sn) which is clearly spherical at scission. In this region (around 132), the TXE curve is minimum, leading to a low value of ν_{tot} (red curve).
- Above the mass 140, the difference Q_{max}-<TKE> seems to be rather constant and consequently, ν_{tot} becomes flat

Prompt Neutron Multiplicities

❑ Prompt neutron multiplicity as a function of pre-neutron mass : <ν>(A)

- At scission: total excitation energy mainly composed of intrinsic excitation energy ($E^{*,SC}_{L,H}$), deformation energy ($E^{Def,SC}_{L,H}$) and collective excitation energy ($E^{Coll,SC}_{L,H}$):

$$\boxed{TXE = E^{*,SC}_{L} + E^{*,SC}_{H} + E^{Def,SC}_{L} + E^{Def,SC}_{H} + E^{Coll,SC}}$$

If nucleons are treated as a Fermi gas: the intrinsic excitation energy can be written as:

$$\boxed{\begin{aligned} E^{*,SC}_{L} &= a_L \left(T^{SC}\right)^2 \\ E^{*,SC}_{H} &= a_H \left(T^{SC}\right)^2 \end{aligned}}$$

where a_L and a_H: level density parameters. Due to the assumed thermodynamic equilibrium at scission, the temperature (T^{SC}) is expected to be the same for both fission fragments.

- Nevertheless, after the acceleration phase of the rotating FF, since the deformation energy is transformed into intrinsic energy (relaxation step), TXE becomes:

$$\boxed{TXE = E^{*}_{L} + E^{*}_{H} + E^{Rot}_{L} + E^{Rot}_{H}}$$

After the full acceleration, temperatures of the light (T_L) and heavy (T_H) fragment, associated to their intrinsic energy, are generally not equal, because deformation of the FF at scission is different.

$$\boxed{\begin{aligned} E^{*}_{L} &= a_L T^2_L \\ E^{*}_{H} &= a_H T^2_H \end{aligned}}$$

FIESTA2017, Sept. 17-22, 2017 | PAGE 26

Note that the several components which appear in the first equation are not known.

The temperatures which governs the intrinsic excitation energy at scission are the same for the two fragments, but become different after the full acceleration.

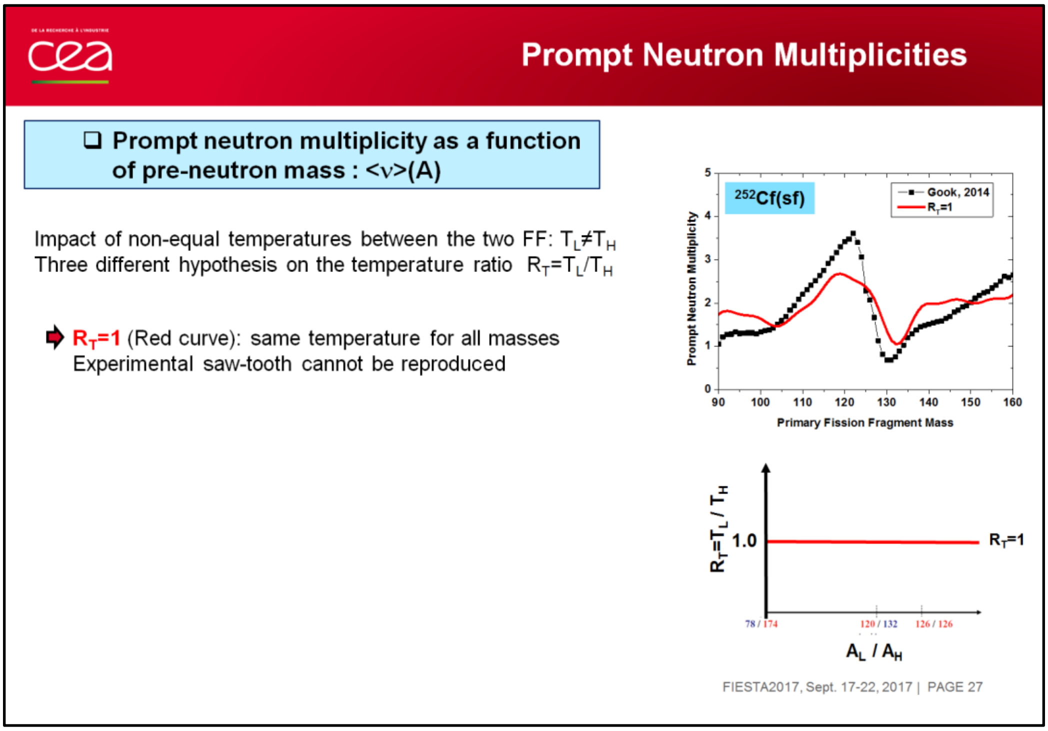

The impact of non-equal temperatures between the two FF has been tested from Monte Carlo simulation (FIFRELIN calculation, Litaize, 2010).

The first case (red curve) corresponds to **R_T=1** (same temperature for all masses). Clearly, with this assumption, the experimental saw-tooth cannot be reproduced.

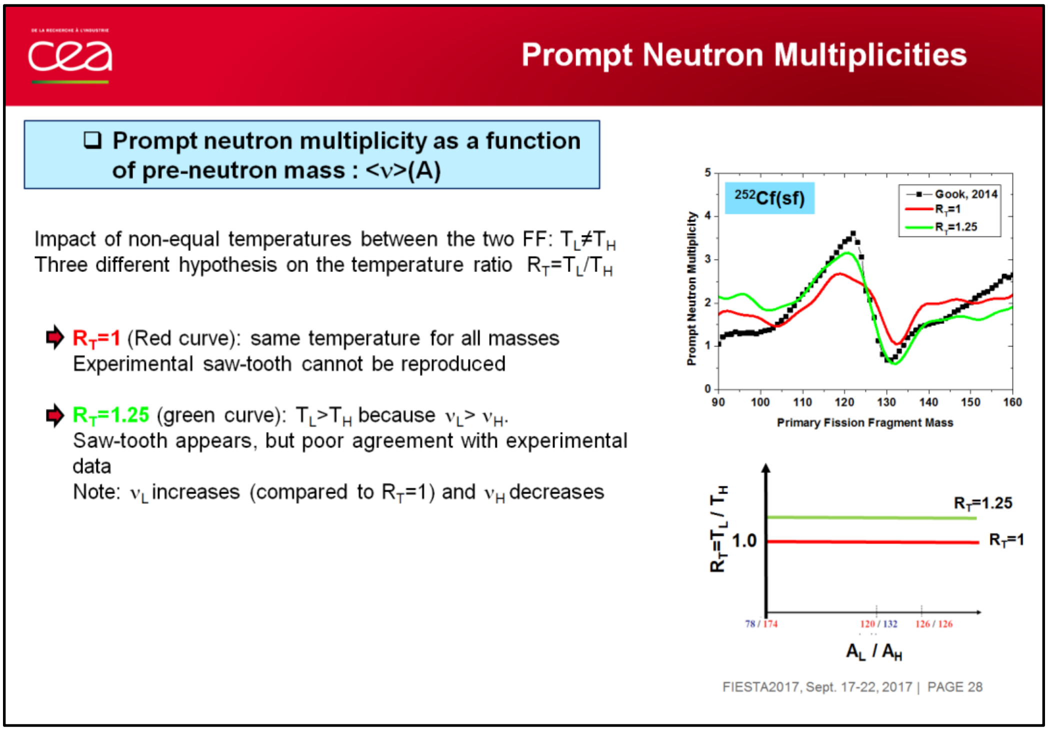

The second case (green curve) corresponds to **$R_T=1.25$**: we assumed here $T_L>T_H$ because we know that $\nu_L> \nu_H$. A saw-tooth appears, but the agreement with experimental data is not vey good. As expected, the neutron multiplicity increases in the light mass region (compared to RT=1) and decreases in the heavy one.

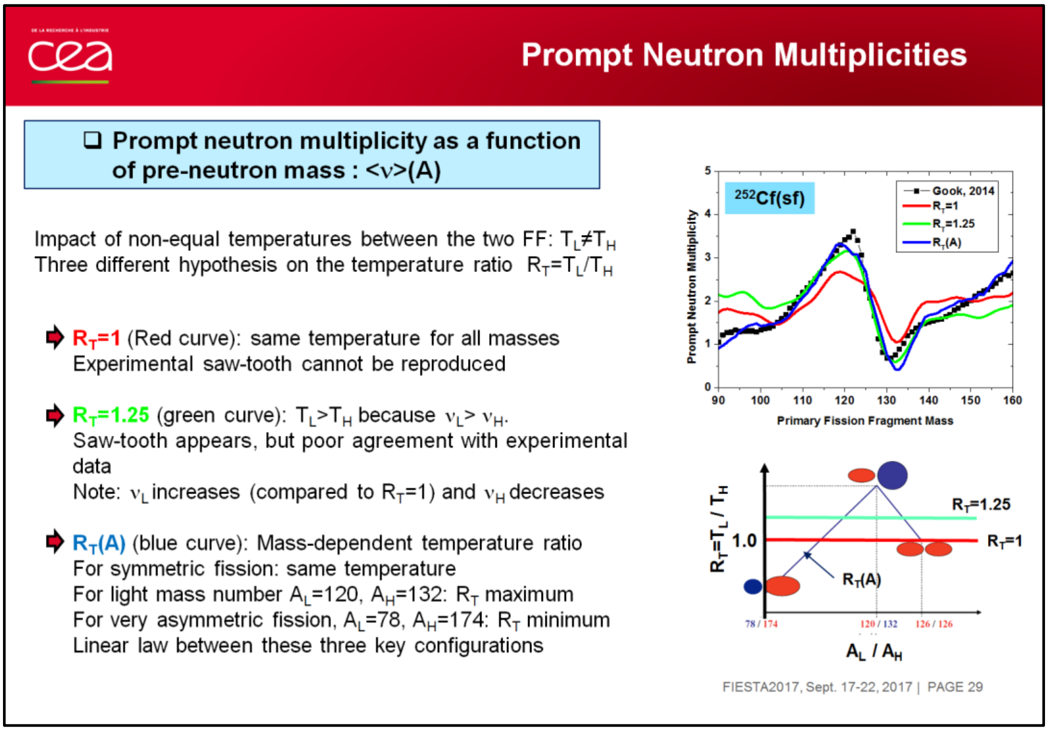

The third case, is a mass-dependent ratio: **$R_T(A)$** (blue curve, bottom). This schematic law was introduced for the following reasons:

For symmetric fission, we expect the same temperature for both complementary fragments and then $R_T=1$. For light mass number $A_L=120$, R_T is maximum because in the case of ^{252}Cf(sf) the complementary heavy fragment is nearly spherical with 132 nucleons. Consequently the light fragment $A_L=120$ gains the major part of the total excitation energy associated with a higher temperature compared to its double magic complementary partner. For very asymmetric fission, the heavy fragment is more deformed than the light fragment because the latter becomes shell stabilized ($Z=28$ and $N=50$), leading to a temperature lower than the temperature of the heavy fragment ($R_T < 1$). A linear law between these three key configurations is assumed to build $R_T(A)$.

With this R_T law, the experimental saw-tooth can be nicely reproduced.

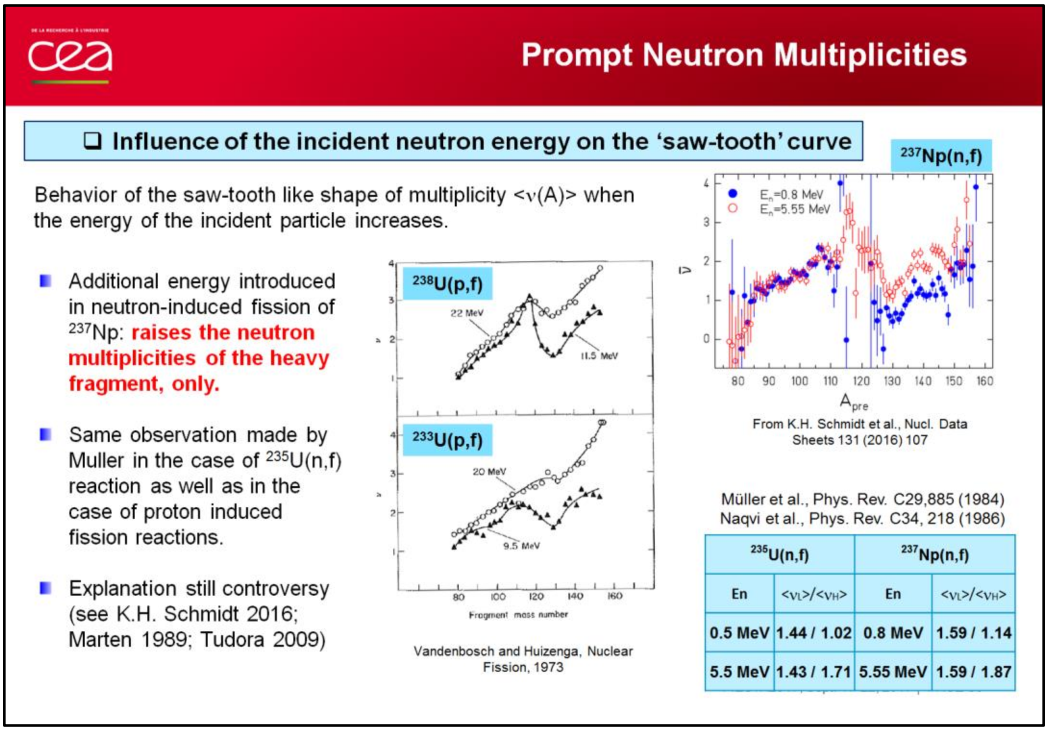

The figure giving results from (p,f) reactions comes from the famous book on fission, written by R. Vandenbosch and J.R. Huizenga: R. Vandenbosch and J.R. Huizenga : "Nuclear Fission" , Academic Press, 1973

From the rare experimental data available, it seems that the increase of the compound nucleus excitation energy leads to an increase of the neutrons emitted by the heavy fragment group.

A mechanism has been proposed by K.-H Schmidt (K.-H. Schmidt and B. Jurado, Phys. Rev. Lett. 104, 212501 (2010)) to explain the sorting of the intrinsic part of the excitation energy. Other models were also proposed to reproduce this observation (see for example: A. Ruben and H. Marten and D. Seeliger, Z. Phys. A, Hadrons and Nuclei, 338, 67-74 (1991) and A. Tudora, Ann. Nucl. Energy 36, 72 (2009)).

This observation probably still needs to be clarified.

Part I: Prompt neutron Emission

- *Angular Distribution of Prompt neutrons*

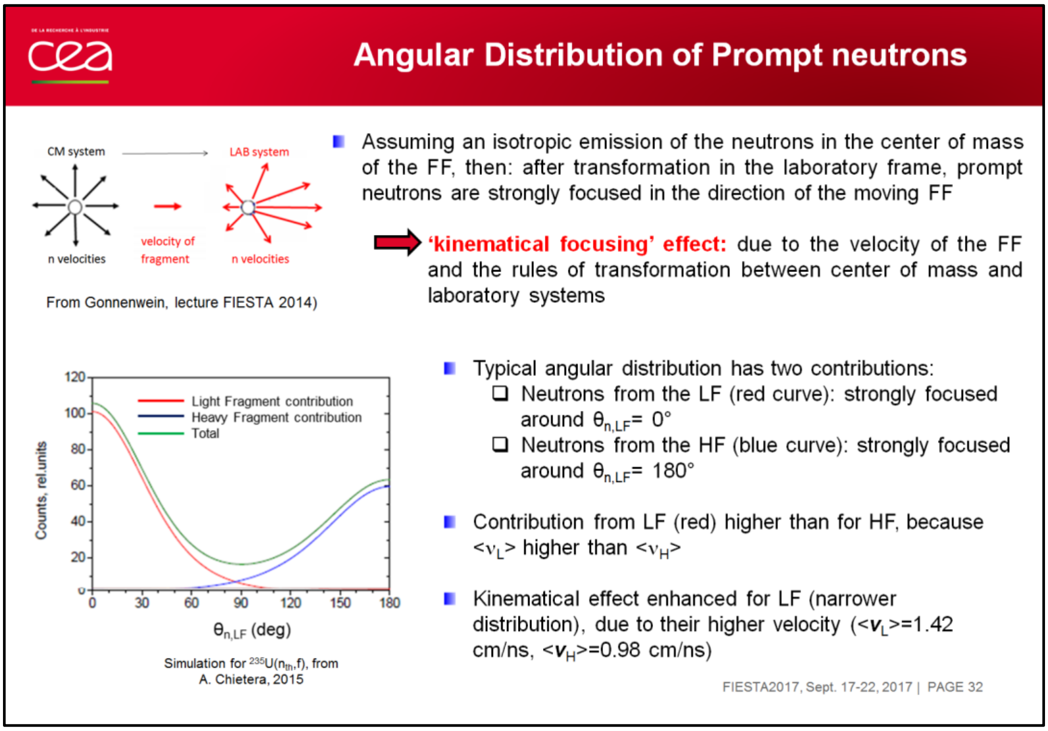

An interesting discussion on this subject can be found in:

A. Chietera, PhD thesis, University of Strasbourg, 2015

See also the pioneering work of Bowman:

H. Bowman et al., Phys. Rev. 126, 2120 (1962)

Angular Distribution of Prompt neutrons

Two additional effects can disturb the angular distribution

① Possible anisotropic emission in the com of the FF may occur due to the angular momenta J (Bowman). Neutrons will preferentially be emitted in the equatorial plane perpendicular to the angular momentum.

Since the spin of the FF is perpendicular to the fission axis, the angular distribution between neutron and fission axis is given by:

$$\boxed{W(\theta_{n,F}) \propto 1 + A_{n,F}\cos^2\theta_{n,F}}$$

$A_{n,F}$= W(0°)/W(90°)-1

$\vartheta_{n,F}$: angle between neutron direction and the fission axis.

The anisotropy in the center of mass system reinforces the kinematical focusing effect

$^{235}U(n_{th},f)$, from A. Chietera, 2015

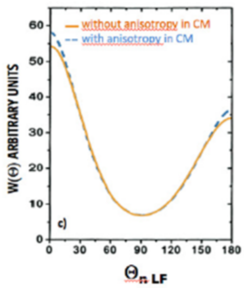

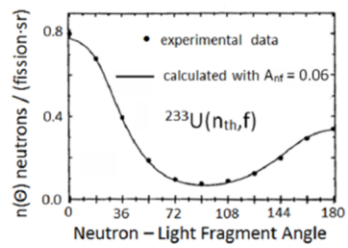

By adding anisotropy in the calculation ($A_{n,F}$=0.06), experimental data nicely reproduced

From A.S. Vorobyev, 2009

FIESTA2017, Sept. 17-22, 2017 | PAGE 33

See also:

J. Terrell, Phys. Rev. 108, 783 (1957)

J. Terrell, Phys. Rev. 113, 527 (1959)

Angular Distribution of Prompt neutrons

② The second effect is due to the possible existence of scission neutrons.

These neutrons are expected to be emit perpendicular to the fission axis.

Monte Carlo calculation of the angular neutron-FF distribution, including scission neutrons shows that scission neutrons will now decrease the kinematic focusing effect.

$^{235}U(n_{th},f)$, from A. Chietera, 2015

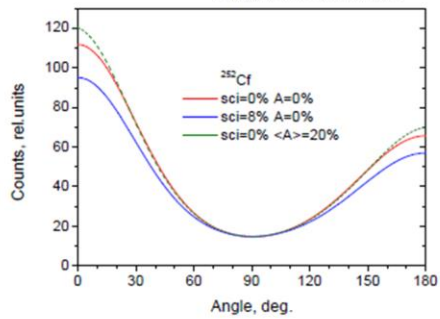

- Both effects (anisotropy due to the spin, existence of scission neutrons) are compensated each others: It is therefore extremely difficult to disentangle each effect separately as shown on this figure.
- An other very promising way to solve this problem is to search for triple coincidence events (n, n, FF).

Part I: Prompt neutron Emission

- *Prompt Fission Neutron Spectrum (PFNS)*
  - Maxwellian
  - Watt
  - Los Alamos Model (LAM)
  - Stochastic approaches

Prompt Fission Neutron Spectrum (PFNS)

❑ Deterministic models used to describe Prompt Fission Neutron Spectra: Maxwellian

- The earliest and simplest model used to describe the Prompt Fission Neutron Spectrum (PFNS), is the single parameter Maxwell-Boltzmann distribution (generally referred to simply as a "Maxwellian"), that depends on a temperature parameter, *T*:

$$N(E) = \left(\frac{2}{\sqrt{\pi}}\right) \times \left(\frac{\sqrt{E}}{T^{3/2}}\right) \exp\left(-\frac{E}{T}\right)$$

- The spectrum is normalized to one and the average energy is given by: $<E>=\frac{3}{2}T$

In the case of ^{252}Cf(sf), the best experimental fit is obtained with T=1.42 MeV, leading to <E>=2.13 MeV.

A comparison between the evaluation of the PFNS performed by Mannhart (1987) with a Maxwellian (with T=1.42 MeV) seems to be surprisingly good, as shown in the figure.

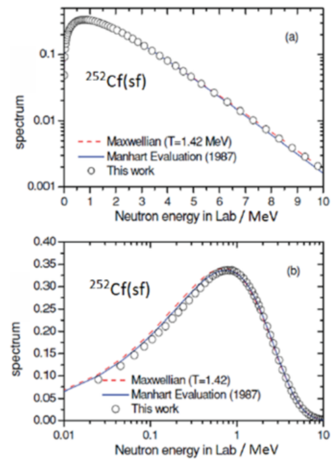

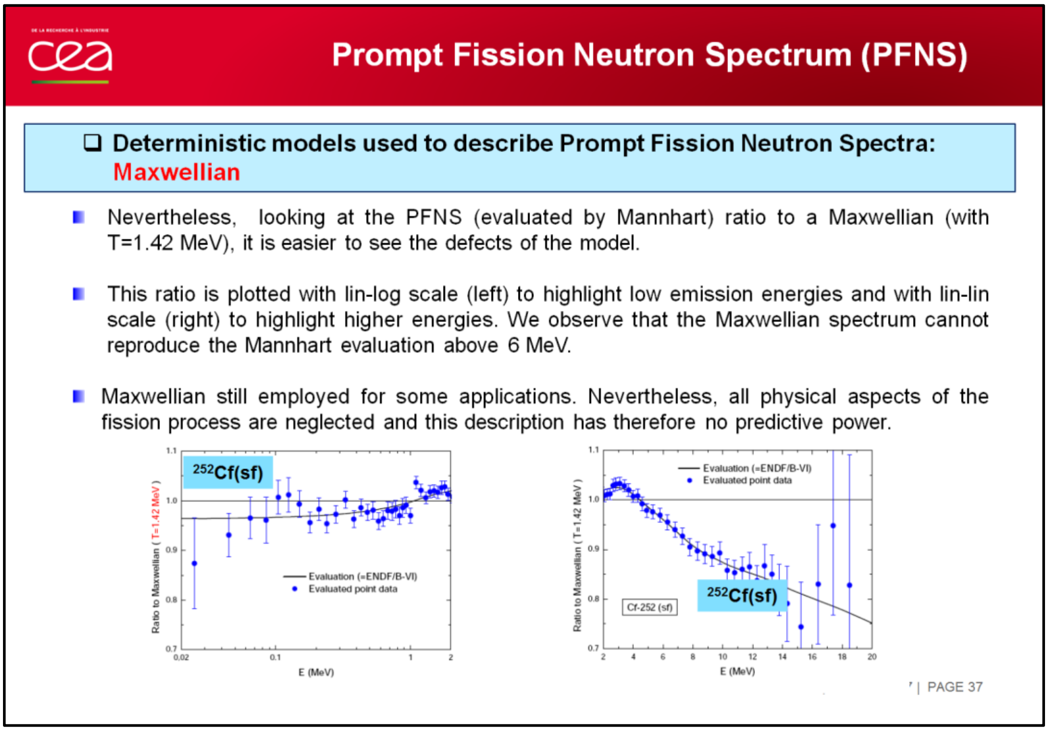

Prompt fission neutron spectrum from 252Cf spontaneous fission is considered as a ‘standard’.

Its evaluation has been performed by Mannhart:

W. Mannhart, in Properties of Neutron Sources, Report IAEA-TECDOC-410 (1987) p. 158.

Note: very often in the literature, the PFNS ratio to a Mawellian is plotted. It is a convenient way to observe the shape and the possible structures of the PFNS.

Prompt Fission Neutron Spectrum (PFNS)

❑ Deterministic models used to describe Prompt Fission Neutron Spectra: WATT

- Watt spectrum has two free parameters: T_W and E_F. (The watt spectrum, in the laboratory system, is obtained from a Maxwell spectrum in the center-of-mass system)

$$\boxed{N(E)=\frac{1}{\sqrt{\pi T_W E_F}}\exp\left(-\frac{E_F+E}{T_W}\right)\times\sinh\left(\sqrt{\frac{4(E_F E)}{T_W^2}}\right)}$$

- The best fit obtained with (for $^{252}Cf(sf)$):
  T_W=0.94 MeV;
  E_F=182 MeV/252 nucleon = 0.72 MeV / nucleon.

- The PFNS average energy is given by: $\boxed{<E>=E_F+\frac{3}{2}T_W}$.
  We obtain: 2.13 MeV

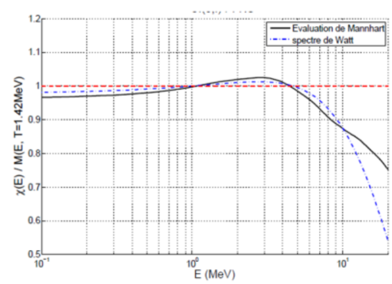

From L. Berge, 2015

- The Watt formulation does account only for the center-of-mass motion of an average fragment. Therefore, the Watt distribution, while more physical than a Maxwellian, still has little predictive power.

The watt spectrum, in the laboratory system, is obtained from a Maxwell spectrum in the center of mass. The transformation is done by considering a single average fragment moving with an average kinetic energy per nucleon Ef.

The figure comes from:

L. Berge, « Contribution à la modélisation des spectres de neutrons prompts de fission. Propagation d’incertitudes à un calcul de fluence cuve », PhD thesis, University Grenoble (France), 2015 (in french)

Prompt Fission Neutron Spectrum (PFNS)

❑ Deterministic models used to describe Prompt Fission Neutron Spectra: Los Alamos model (LAM)

- Los Alamos Model proposed by Madland and Nix in 1982
- Prompt fission neutrons assumed to be emitted from the fully accelerated FF
- In the center of mass of the FF, the evaporation spectrum of prompt neutrons follows a Weisskopf spectrum:

$$\text{(1)} \quad \boxed{\begin{aligned} \phi(\varepsilon,T) &= \mathrm{k(T)}\,\sigma(\varepsilon)\,\varepsilon\,\exp(-\varepsilon/\mathrm{T}) \\ \mathrm{k(T)} &= \left(\int_0^\infty d\varepsilon\,\sigma(\varepsilon)\,\varepsilon\,\exp(-\varepsilon/\mathrm{T})\right)^{-1} \end{aligned}}$$

ε: center-of-mass neutron kinetic energy
T: residual nuclear temperature after neutron emission
$\sigma(\varepsilon)$: cross section for the inverse process of compound nucleus formation through neutron capture
k(T): normalisation constant

Note: if $\sigma(\varepsilon)$ constant, then $\boxed{\phi(\varepsilon,T) = \dfrac{\varepsilon}{\mathrm{T}^2}\exp(-\varepsilon/\mathrm{T})}$

Note: To calculate the average spectrum of all neutrons emitted from all FF, Eq. (1) needs to be folded with a distribution of fission fragment temperatures or excitation energies.

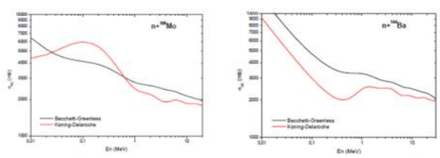

Examples of cross section $\sigma(\varepsilon)$ for the inverse process of compound nucleus for two complementary FF

FIESTA2017, Sept. 17-22, 2017 | PAGE 39

The Los Alamos Model has been extensively used for the evaluations of PFNS which can be found in the international nuclear data libraries (ENDF/B, JEFF, JENDL…).

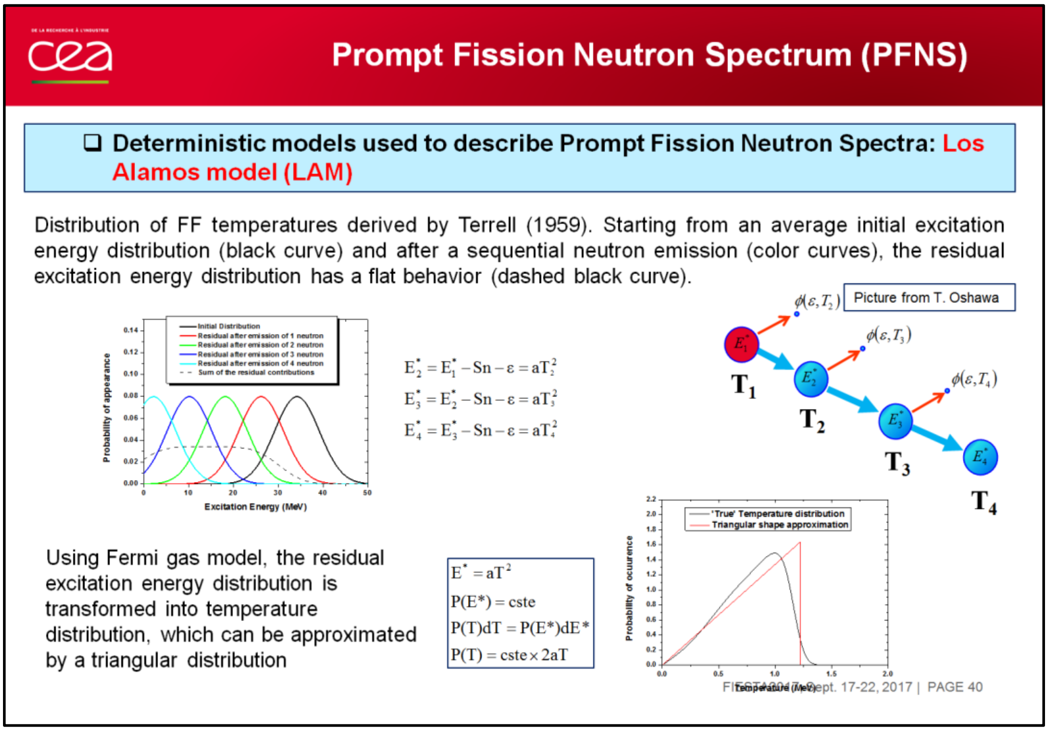

The distribution of residual fission fragment temperature is derived as follows:

Terrell (1959) observed that from an average initial excitation energy distribution (black curve) and after a sequential neutron emission (color curves), the residual excitation energy distribution has a flat behavior (dashed black curve).

This residual excitation energy distribution was used to obtain a temperature distribution based on the Fermi gas model (black curve, bottom plot). As illustrated on this figure, the residual temperature distribution can be reasonably well described by a triangular distribution (red curve).

Prompt Fission Neutron Spectrum (PFNS)

❑ Deterministic models used to describe Prompt Fission Neutron Spectra: Los Alamos model (LAM)

$$P(T)=\begin{cases}2T/T_{\max}^2 & (\mathrm{T}\le\mathrm{T}_{\max})\\ 0 & (\mathrm{T}\le\mathrm{T}_{\max})\end{cases}$$

Residual nuclear temperature distribution (triangular form) is used in the LAM, with

$\mathrm{T}_{\max}^2 = <E^*>/a$ 'a' is the level density parameter approximated by: $a=A_{CN}/11$ (in the initial model proposed by Madland and Nix, 1982) and <E*>=<TXE>=<Q>+En+Bn-<TKE>

The prompt fission neutron spectrum, in the center of mass system, is then given by folding Eq.(1) over the residual temperature distribution:

$$\Phi(\varepsilon)=\int_0^{\infty}\mathrm{dT}\,\mathrm{P(T)}\,\phi(\varepsilon,T)$$

$$\Phi(\varepsilon)=\frac{2\sigma(\varepsilon)}{T_{\max}^2}\int_0^{T_{\max}}\mathrm{dT}\,\mathrm{k(T)}\,\mathrm{T}\exp(-\varepsilon/\mathrm{T})$$

By considering the two complementary FF, we get:

$$\Phi(\varepsilon)=\frac{1}{2}\left[\Phi(\varepsilon,\sigma_c^L)+\Phi(\varepsilon,\sigma_c^H)\right]$$

$$\text{with }\Phi(\varepsilon,\sigma_c^L)=\int_o^{T_{\max}}\phi(\varepsilon,\sigma_c^L)P(T)dT$$

The neutron energy spectrum $N(E,E_f)$ in the laboratory system for a fission fragment moving with average kinetic energy per nucleon E_f is obtained by:

$$N(E)==\frac{1}{2}\left[N(E,E_f^L,\sigma_C^L)+N(E,E_f^H,\sigma_C^H)\right]$$

with:

$$\begin{aligned}&N(E,E_f,\sigma_c)\\&=\frac{1}{4\sqrt{E_f}}\int_{(\sqrt{E}-\sqrt{E_f})^2}^{(\sqrt{E}+\sqrt{E_f})^2}\left[\frac{\Phi(\epsilon,\sigma_c)}{\sqrt{\epsilon}}\right]d\epsilon\\&=\frac{1}{2\sqrt{E_f}T_m^2}\int_{(\sqrt{E}-\sqrt{E_f})^2}^{(\sqrt{E}+\sqrt{E_f})^2}\sigma_c(\epsilon)\sqrt{\epsilon}\,d\epsilon\int_0^{T_m}c(T)\,T\exp(-\epsilon/T)\,dT\end{aligned}$$

The average kinetic energy per nucleon of the average light fragment A_L and average heavy fragment A_H are obtained using momentum conservation :

$$E_f^{L,H}=(A_{H,L}/A_{L,H})(\langle E_f^{tot}\rangle/A)$$

Prompt Fission Neutron Spectrum (PFNS)

❑ **Deterministic models used to describe Prompt Fission Neutron Spectra: Los Alamos model (LAM)**

The figure (top) shows PFNS ratio to a Maxwellian with T=1.42 (green curve), where the PFNS is calculated with the original LAM

Note: average energy of PFNS given by: $\boxed{\langle E \rangle = \frac{1}{2}(E_f^L + E_f^H) + \frac{4}{3}T_m}$

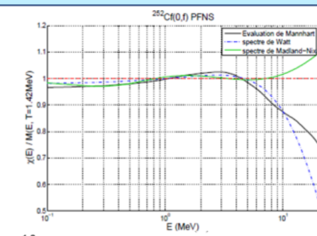

Improvements of LAM recently proposed (see Madland 2017, Hambsch 2005, Tudora 2009):

- ❑ Temperatures of the light and heavy fragment not equal
- ❑ Contributions of the light and heavy fragments to the total PFNF are weighted according to their multiplicity
- ❑ Triangular form of P(T): changed by a more realistic form
- ❑ Anisotropic emission in the center of mass introduced
- ❑ Level density parameters specific for the LF and the HF
- ❑ Fission modes incorporated (Brosas'model 1990)

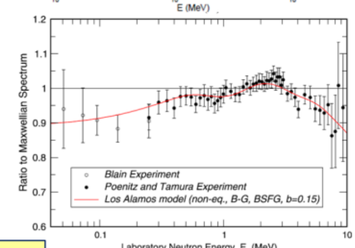

Hambsch, 2005

All these modifications allow a much better description of PFNS

FIESTA2017, Sept. 17-22, 2017 | PAGE 42

Note: the extension of the LAM proposed by Vladuca and Tudora leads to the so-called 'Point-By-Point' model (PbP): For a given fissioning nucleus, instead of considering one fission fragment pair (the most produced one), as initially done by Madland, all FF pairs are considered.

See:

G. Vladuca and A. Tudora, Comput. Phys. Commun. 125 (1–3), 221–238 (2000)

A. Tudora, Ann. Nucl. Energy 36, 72 (2009)

Prompt Fission Neutron Spectrum (PFNS)

❑ Stochastic approaches

Several Monte-Carlo codes have been developed recently aiming at: calculating fission observables (PFNS, PFGS, prompt neutron and gamma multiplicities….) and searching for correlations between these observables.

Simulation performed in two steps:

(i) sampling of FF characteristics (A, Z, KE, E*, J, π)

(ii) simulating the deexcitation of both fission fragments

- Code **FREYA,** developed through a collaboration between LLNL and LBNL: Available for downloading
  (Vogt, 2009; Vogt, 2011; J. Randrup, 2009; Vogt, 2012, Verbeke, 2015; Vogt, 2014; Wang, 2016)
- Code **CGMF,** developed at LANL (USA)
  (Talou, 2011; Talou, 2013; Stetcu, 2014; Becker 2013; Lemaire, 2005; Lemaire, 2006)
- Code **FIFRELIN**, developed at CEA-Cadarache (France)
  (Litaize, 2010; Serot, 2014, Litaize, 2015; Regnier, 2016;)
- Code **GEF**, developed at CENBG (France): Available for downloading
  (Schmidt, 2010; Schmidt, 2011; Schmidt, 2016)

In recent years, several Monte-Carlo codes have been developed, aiming at calculating fission observables (PFNS, PFGS, prompt neutron and gamma multiplicities….) and aiming at searching for correlations between these observables. Usually, the simulation is performed in two steps: (i) the first step consists in the sampling of FF characteristics (mass, nuclear charge, kinetic energy, excitation energy, spin and parity π; (ii) the second step consists in simulating the deexcitation of both fission fragments.

The event-by-event Monte Carlo fission code **FREYA** (Fission Reaction Event Yield Algorithm) has been developed through a collaboration between LLNL and LBNL. It simulates the entire fission process and produces complete fission events with full kinematic information on the emerging fission products and the emitted neutrons and photons, incorporating sequential neutron and photon evaporation from the fission fragments. FREYA is available for downloading.

The **CGMF** code represents a merger of two codes previously developed at LANL: FFD, which performed Monte Carlo simulations of fission fragments following the Weisskopf-Ewing statistical theory, and CGM, a Monte Carlo Hauser-Feshbach code not initially developed for treating fission events. A new version of CGMF is being developed, treating both fission and non-fission events naturally.

The **FIFRELIN** code has been developed at CEA-Cadarache (France) with the aim of calculating the main fission observables, and in particular the energy spectra and multiplicities of the emitted prompt particles. In the first version of the code, prompt neutron emission was simulated using a Weisskopf spectrum. In a more recent version, the de-excitation of the fission fragments is treated by using the Hauser-Feshbach formalism.

The **GEF** code has been developed at CENBG (France) with the aim of calculating all the main fission observables (isobaric, isotopic and isomeric yields, energy and multiplicity of prompt particles,… The de-excitation of the FF is obtained within the statistical model, using neutron and gamma widths from systematic. GEF is available for downloading.

Prompt Fission Neutron Spectrum (PFNS)

❑ Stochastic approaches

- FF deexcitation simulated from statistical Hauser-Feshbach model (CGMF and FIFRELIN codes): accounts for the conservation of energy, spin and parity of the initial and final states.

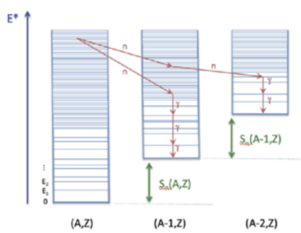

From R. Capote, 2016

Neutron width (for a given neutron orbital momentum l and total angular momentum j): determined from the neutron transmission coefficients ($T_{l,j}$)

$$\Gamma_n(\varepsilon_n, l, j) = \frac{T_{l,j}(\varepsilon_n)}{2\pi\,\rho(E_i, J_i, \pi_i)}$$

Gamma width (for a transition of type X = E,M and multipolarity L): computed via gamma strength function $f_{XL}(\epsilon_\gamma)$

$$\Gamma_\gamma(\varepsilon_\gamma, XL) = \frac{f_{XL}(\varepsilon_\gamma)\varepsilon_\gamma^{2L+1}}{\rho(E_i, J_i, \pi_i)}$$

Probability of a neutron emission Pn: Competition between neutron and γ accounted for

$$P_n = \frac{\Gamma_n}{\Gamma_n + \Gamma_\gamma}$$

- In FREYA code: neutron emission simulation based on Weisskopf evaporation model.

FIESTA2017, Sept. 17-22, 2017 | PAGE 44

In order to calculate neutron and gamma widths, the following key ingredients are needed (see equations):

❑ Level density models: ρ

❑ Optical models, from which neutron transmission coefficients T can be calculated and neutron widths deduced

❑ Strength function models f, from which gamma widths can be calculated

All these models (and their recommended parameters) are reminded in detail in the following reference:

R. Capote, et al., Nucl. Data Sheets 110, 3107 (2009)

Other important references are:

V.F. Weisskopf, Phys. Rev. 52, 295 (1937)

W. Hauser and H. Feshbach, Phys. Rev. 87, 366 (1952)

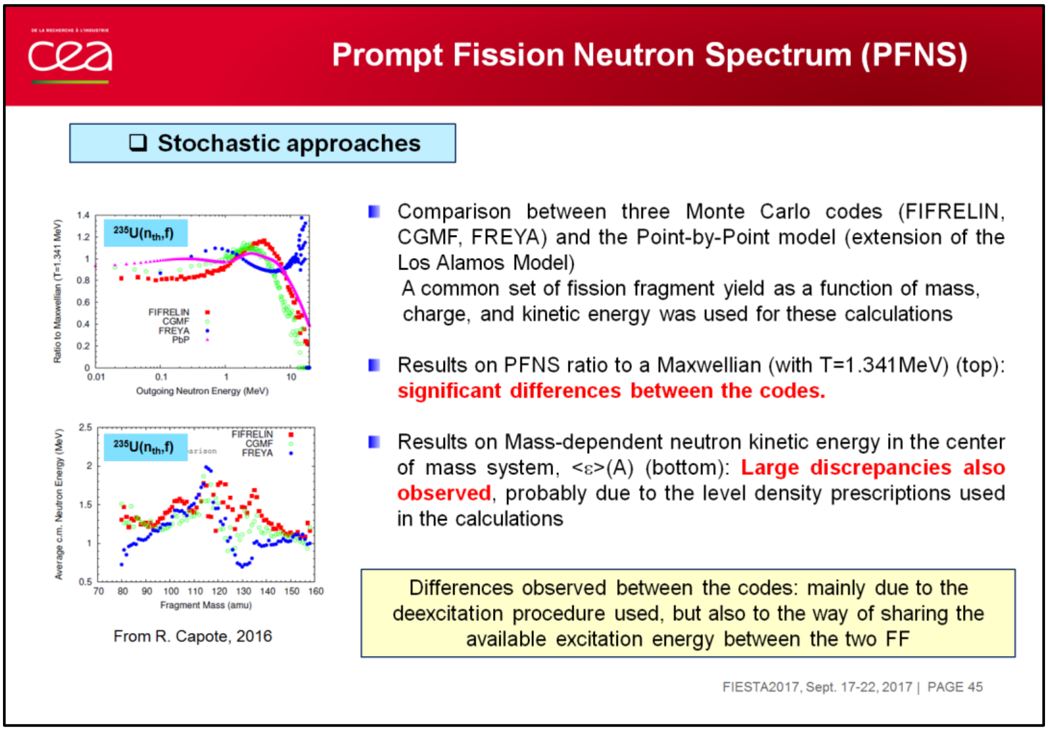

As explained in the paper of R. Capote (R. Capote, et al., Nucl. Data Sheets 131, 1 (2016), results obtained from the three Monte Carlo codes were performed using a common set of fission fragment yield as a function of mass, charge, and kinetic energy. In this way, the inter comparison between the codes is more pertinent. Note that the calculation from the PbP model (extension of the Los Alamos Model) is also included in the plot. On the figure (top), PFNS ratio to a Maxwellian (with T=1.341 MeV) are plotted, showing significant differences between the codes. It must be emphasized that none of them can reproduce satisfactory the experimental data. It can be also due to the fact that additional neutron sources (scission neutrons ?) have to be incorporated.

Predictions relative to the mass-dependent neutron kinetic energy in the center of mass system, <ε>(A), are shown (bottom). Again, large discrepancies are observed, probably due to the different level density prescriptions used in the calculations.

Part II
Prompt gamma Emission

- *Time scale for prompt and 'late' gamma emission*
- *Available Energy for Prompt gamma Emission*
- *Prompt Fission Gamma spectrum (PFGS)*
- *Prompt Fission Gamma-ray Multiplicity*

Time scale for prompt and 'late' gamma emission

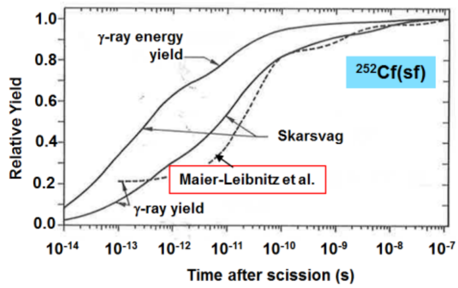

The relative yields of γ-rays and γ-ray energy as a function of time after scission plotted (top): All curves are normalized at time of 1.2×10^{-7}s after scission

Straight lines: measurement performed by Skarsvag
Dashed line: evaluation made by Maier-Leibnitz

Note. The total photon energy increases faster with time than the total number of photons: reflects the fact that early gammas have higher energies.

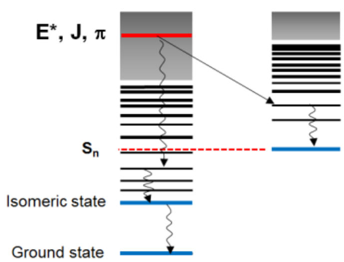

- **According to Skarsvag: more than 90% of the γ-rays are emitted prior to 1ns.**
- The earliest gammas appear at about 10^{-14} s after scission
- The bulk of prompt gammas is emitted within 100 ns
- 'Late' gammas can be emitted by fragments up to about 1 ms: from **isomeric states** which can be populated during the deexcitation of the fission fragments

Figure comes from:

H.-H. Knitter, et al., in "The Nuclear Fission Process", C. Wagemans ed., CRC Press 1991

Available Energy for Prompt gamma Emission

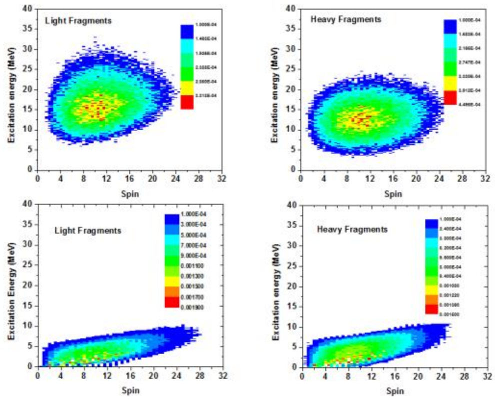

- Example of Monte Carlo calculation showing the (E*,J) distributions for the LF (left) and the HF (right), before prompt neutron emission (top) and after prompt neutron emission (bottom).
- Gives an idea of the average remaining energy available to emit prompt γ-rays.

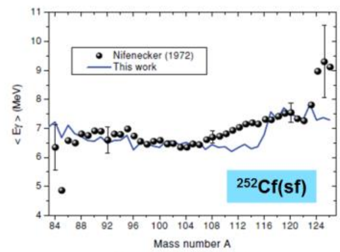

Litaize and Serot, 2010

- Average excitation energy <Eγ>(A) available for the two complementary FF to emit prompt γ-rays: <Eγ>(A) plotted as a function of the light fragment mass shows a rather flat behavior (right figure).

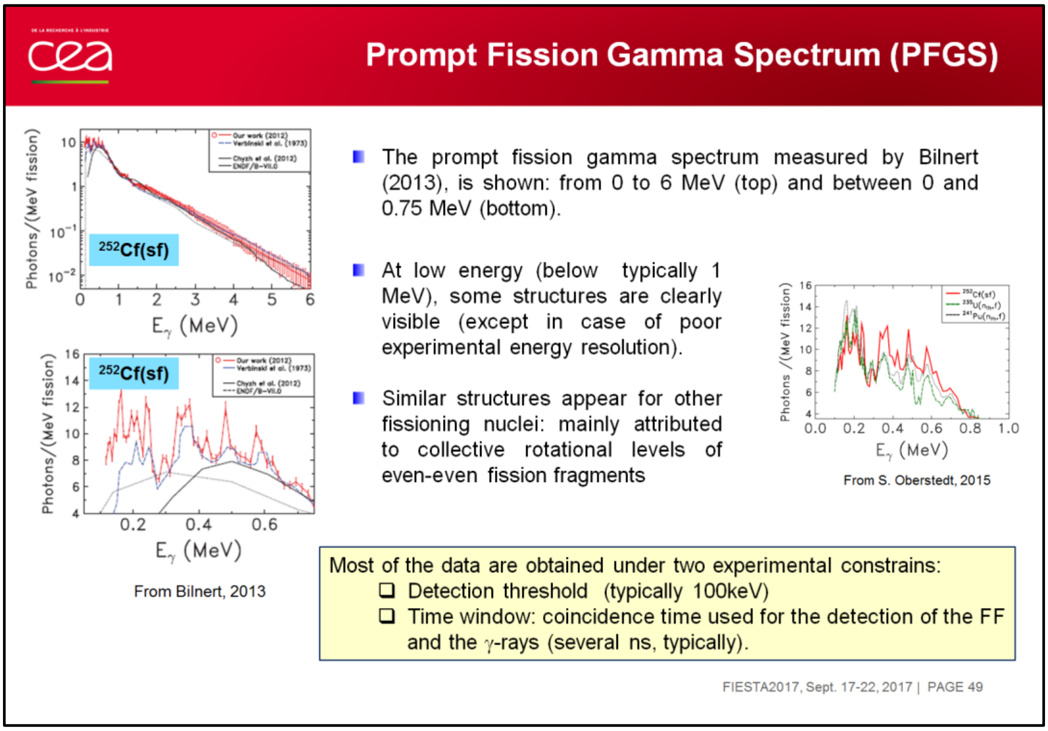

Most of the experimental data were obtained under mainly two experimental constrains:

- ❑ Detection threshold (typically 100 keV)
- ❑ Time window, which corresponds to the coincidence time window used for the detection of the FF and the γ-rays (several ns).

These two parameters can (and must) be taken into account by the Monte Carlo codes for comparison with experimental data. The first one by simply not recording events below the energy threshold, the second one by accounting for the half life of nuclear levels.

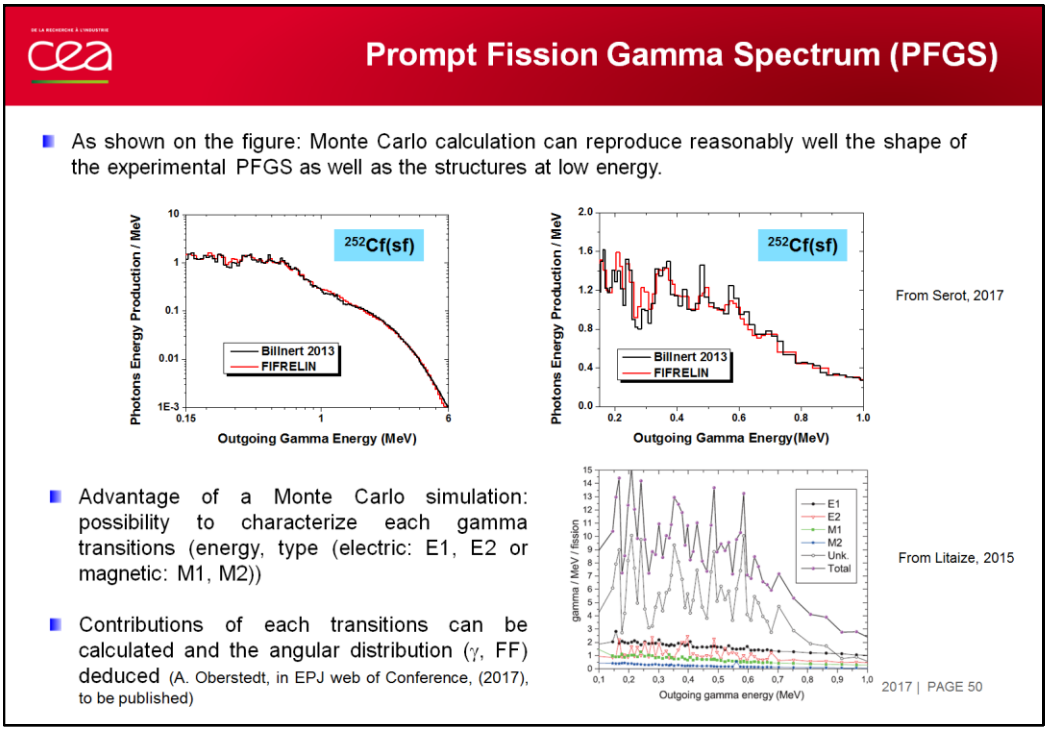

One of the main advantage of a Monte Carlo simulation is the possibility to characterize each gamma transitions: energy, type (electric: E1, E2 or magnetic: M1, M2)). Hence, contributions of each transition can be calculated and the angular distribution (γ, FF) deduced (see, for example: A. Oberstedt, in EPJ web of Conference, (2017), to be published).

Prompt Fission Gamma Spectrum (PFGS)

In the case where Monte Carlo codes describes the deexcitation of the FF from Hauser-Feshbach theory: level density and the strength function models have an impact on the calculated PFGS. Good experimental data can be therefore used to test the models.

Example:

Calculation 1 (black curve): Composite Gilbert Cameron (CGCM) model for the level density, and Enhanced Generalized LOrentzian model (EGLO) for the photon strength function

Calculation 2 (red curve): tabulated values from HFB calculations for the level density, and tabulated values from microscopic calculations (noted HF+BCS+QRPA) for the photon strength function

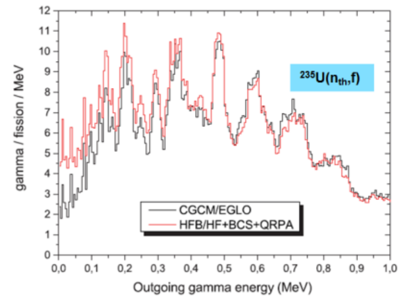

From O. Litaize, private communication

➡ Below around 200 keV, calculation 1 predicts a lower gamma multiplicity.

Accurate measurement of PFGS can be therefore a good test of the level density and strength function models

Prompt Fission Gamma-ray Multiplicity

- Mass-dependent average prompt gamma multiplicity: $\langle M\gamma \rangle (A)$
Measured for ^{252}Cf(sf) (top) and for ^{235}U(n_{th},f) (bottom)

- Note: for ^{252}Cf(sf), except in the mass region around 132, a rather flat behavior is observed. It is not the case for ^{235}U(n_{th},f) reaction, where a saw-tooth shape appears (similar as for prompt neutron multiplicity)

- Monte Carlo simulations (blue curves): exhibit a rather flat behavior, except in the [125–135] mass region (lower gamma multiplicity related to near spherical nuclei)

Simulations impacted by the spin distribution of the FF after prompt neutron emission, which are unfortunately poorly known (big experimental challenges)

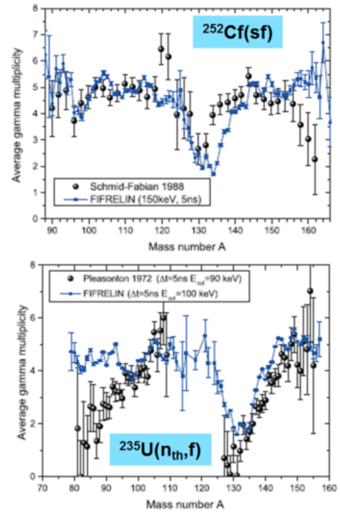

From O. Litaize, 2015

Prompt Fission Gamma-ray Multiplicity

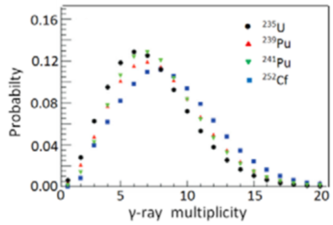

Fom Gonnenwein, lecture given at FIESTA 2014

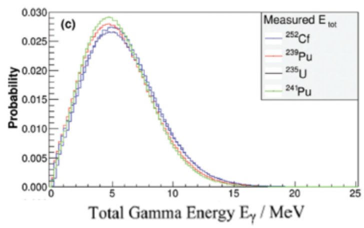

From Chyzh, 2014.
The γ-ray energy was measured with the spectrometer DANCE from LANSCE in a time window of 40 ns after fission.

- Prompt gammas contribute to the heating of reactor cores: ⇒ precise knowledge of the energy release by gamma emission required for reactor applications
- Strong experimental efforts done during last years
- Prompt γ-ray multiplicity distribution (normalized to one): Similar distributions for various fissioning systems (top) Up to 20 γ-quanta per fission can be detected !
- γ-ray energy distributions (bottom): also very similar behavior for various fissioning nuclei

Examples of average quantities: $\langle M\gamma \rangle$, $\langle E\gamma \rangle$ and $\langle \varepsilon_\gamma \rangle$ (table), including experimental detection parameters

$^{235}U(n_{th},f)$	ΔE	Δt	$\langle M_\gamma \rangle$	$\langle \varepsilon_\gamma \rangle$	$\langle E_\gamma \rangle$
	MeV	ns		MeV	MeV
Verbinski 1973:	0.14-10.0	10	6.7(3)	0.97(5)	6.5(3)
Chyzh 2013:	0.15-9.5	100	6.95(30)	1.09	7.57
Oberstedt 2013:	0.1-6.0	~ 10	8.19(11)	0.85(2)	6.92(9)
$^{252}Cf(sf)$	ΔE	Δt	$\langle M_\gamma \rangle$	$\langle \varepsilon_\gamma \rangle$	$\langle E_\gamma \rangle$
Verbinski 1973:	0.14-10.0	10	7.8(3)	0.88(4)	6.84(30)
Skarsvag 1980:	> 0.114	12	9.7(4)	0.72	7.0(3)
Chyzh 2012:	0,15-9.5	10	8.15	0.96	7.8
Billnert 2013:	0.1–6.0	<1.5	8.3(1)	0.80(1)	6.64(8)

Fom Gonnenwein, lecture given at FIESTA 2014

Part III
Delayed neutron and Gamma Emission

- *Origin of the delayed neutron and gamma emission*
- *Main precursors*
- *Examples of delayed neutron and gamma spectra*
- *Influence of incident neutron energy on DN multiplicity*

Origin of the delayed neutron and gamma emission

Delayed neutrons emitted by the fission products several seconds or even minutes after the fission are of crucial importance for the **control and the safety of nuclear reactors**. Accurate knowledge data on delayed neutron characteristics are therefore requested by nuclear industry.

- **Delayed neutron precursors:** Fission products that emit delayed neutrons
- Almost all FPs are neutron-rich β^- emitters. This β^- emission can leave the daughter nucleus into an excited state, with sufficient energy available to emit a neutron: (β^-, n) disintegration
- These neutrons are called **delayed neutrons**. Their 'delay' is linked to the lifetime of the β- decay: typically: from milliseconds to several hundred seconds
- Probability to emit a neutron after a β- decay: Pn; Corresponds to the branching ratio: Pn = (β^-,n) / β^-
- After a β- decay or a (β-,n) decay: the daughter nucleus can reach its ground state by γ-ray emission ⟹ **'delayed' gamma**

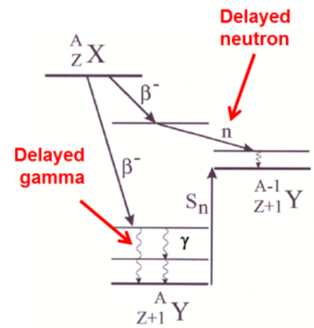

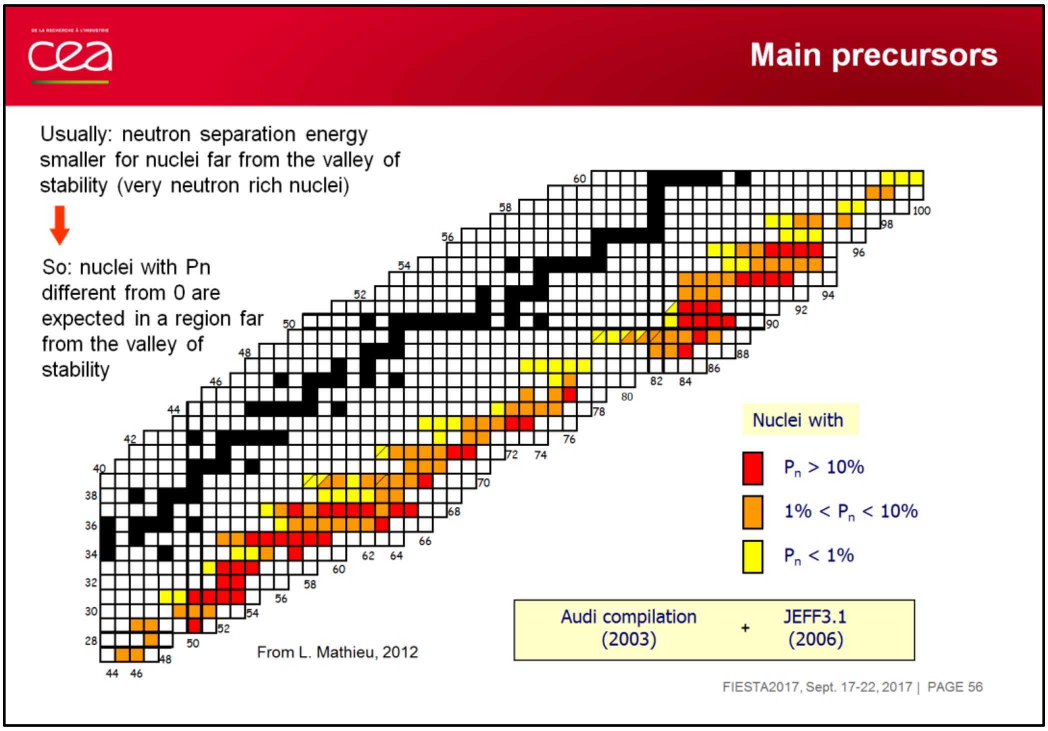

This figure is taken from:

L. Mathieu et al., JINST 7 P08029 (2012)

Main precursors

- Delayed neutron multiplicity generally given in pcm (percent mille)
- Examples of average multiplicity $<\nu_{del}>$ for various fissioning nuclei (Table 1)
- Example of contribution of the main precursors to the total delayed neutron multiplicity (Table 2, $^{235}U(n_{th},f)$ reaction)

Table 1 (from JEFF Report 20, NEA OECD, 2009)

Reaction	$< \nu_{del} >$ (pcm)
n+^{235}U (En=thermal)	1654 ± 2.5 %
n+^{238}U (En=400 keV)	4511 ± 1.3 %
n+^{239}Pu (En=thermal)	624 ± 3.8 %
n+^{240}Pu (En=400 keV)	960 ± 11.4 %
n+^{241}Pu (En=thermal)	1560± 10.2 %
n+^{242}Pu (En=400 keV)	2280 ± 11.0 %

Table 2

Precursor	Contribution (%)
^{137}I	14.6
^{89}Br	11.7
^{94}Rb	9.3
^{90}Br	7.9
^{88}Br	7
^{85}As	5.6
^{138}I	4.8
^{98m}Y	4.6
^{95}Rb	3.7
^{139}I	3.7

Main precursors

- For nuclear energy applications: delayed neutrons usually described by using 8 universal groups
- Each group characterized by an average half lives (Table 3)
- For a given fission reaction: abundance of each group is needed to calculate the time-dependent delayed neutron multiplicity (figure below)

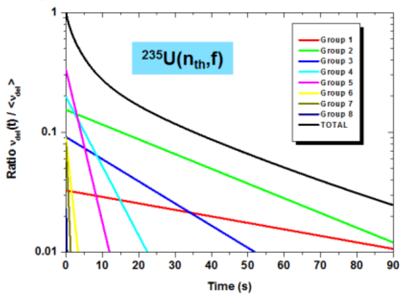

Table 3, $^{235}U(n_{th},f)$, NEA-WPEC6, 2002

Group Number	Main Precursors	Half-life (s)	Group Average Half-lives (s)	Abondance
1	Br-87	55.6	55.6	(3.28 ± 0.42) %
2	I-137	24.5	24.5	(15.40 ± 0.68) %
3	Br-88	16.3	16.3	(9.14 ± 0.90) %
4	I-138 Rb-93 Br-89	6.46 5.93 4.38	5.21	(19.7 ± 2.3) %
5	Rb-94 I-139 As-85 Y-98	2.76 2.30 2.08 2.00	2.37	(33.1 ± 0.66) %
6	Kr-93 Cs-144 I-140	1.29 1.00 0.86	1.04	(9.03 ± 0.45) %
7	Br-91 Rb-95	0.542 0.384	0.424	(8.12 ± 0.16) %
8	Rb-96 Rb-97	0.203 0.170	0.195	(2.29 ± 0.95) %

Examples of delayed neutron and gamma spectra

The figures below represent: a delayed gamma spectrum measured at 1000 s after fission (left) and a delayed neutron spectrum of the ^{89}Br (one of the main precursor)

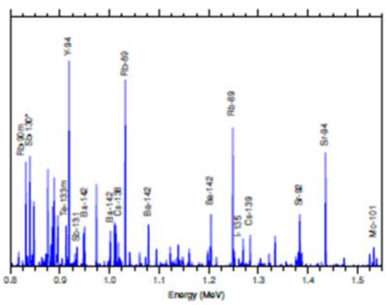

Delayed γ-ray spectrum for ^{235}U at 1000 seconds. Some precursors can be clearly identified (From T.K. Lane, 2015)

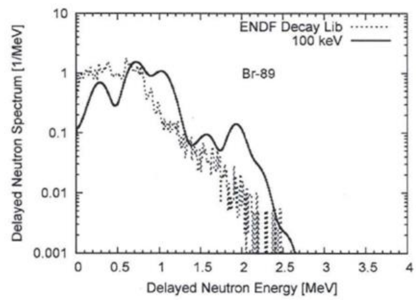

Delayed neutron energy spectrum of the ^{89}Br Given in the ENDF/decay data library and calculated within QRPA-Hauser-Feshbach model (From T. Kawano, 2008)

Influence of incident neutron energy on DN multiplicity

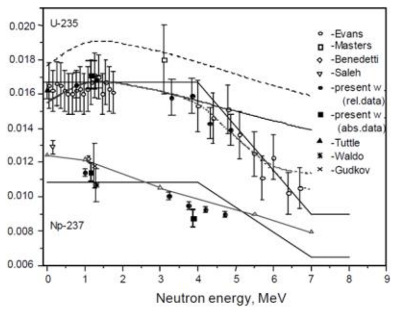

From NEA/WPEC-6 Report (2002)

- We know that by increasing the energy of the incident neutron, fission product yields become higher in the symmetric mass region.
- Yet, in this symmetric mass region, neutron precursors are fewer.
- Therefore, the total average delayed neutron multiplicity is expected to decrease when incident neutron energy grows. This is illustrated on the figure, where the total delayed neutrons yields for neutron-induced fission of ^{235}U and ^{237}Np are plotted.

Conclusion

- Very early after the discovery of nuclear fission, a report on the observation of fission neutrons has been published (H. von Halban et al., Nature 143, 470 (1939); O. Hahn and F. Strassmann: Naturwiss. 27, 89 (1939))

- Due to their importance for nuclear applications, the main characteristics of the prompt neutron and prompt gamma were investigated by the experimentalists and the theoreticians.

- It is generally accepted that the main contribution of the prompt neutron emission is coming from the evaporation of the fully accelerated fission fragments. Nevertheless, it seems that an additional neutron source, which could be the scission neutrons, is needed to describe the main prompt neutron properties.

- After prompt neutron emission, the FF released the remaining excitation energy by gamma emission (neglecting the n/γ competition). Due to their importance for reactor applications, strong experimental efforts have been made in the last years, to improve our knowledge of the prompt gamma properties (multiplicity, spectra).

- Monte Carlo codes have been recently developed aiming at calculating fission observables (PFNS, PFGS, prompt n and g multiplicities….) and searching for correlations between these observables.

Conclusion

- Still some open questions and some nuclear data are still highly requested

  - Knowledge of the spin distributions acquired by the FF, which are highly desired to simulate in particular the prompt fission gamma properties:
    - Mechanism used during the fission process to generate the FF spins: still not clear
    - Experimental spin distributions are needed

  - How the available excitation energy at scission is shared between the two fragments ?
    Experimental correlations between fission observables are strongly requested for answering this question: it gives constraints to the models…
    (good example: correlations between neutrons and γ multiplicities as shown by P. Talou, 2013)

  - Existence of scission neutrons: still an open question. Measure in triple coincidences (n, n, FF) may be a nice way to answer

  - Pre-neutron mass and charge yields and pre-neutron kinetic energy are needed for additional fissioning nuclei and for higher incident neutron energies: very important for Monte Carlo calculations

  - Prompt n and γ experimental data: still scarce at high incident neutron energy. Needed for testing the models and for nuclear energy applications

References

Some plots shown in this document and discussions about prompt neutron and gamma emission come from lectures given by F. Gonnenwein:
F. Gonnenwein, lecture given at Ecole Joliot-Curie, 2014
F. Gonnenwein, lecture given at FIESTA-2014

Some references on scission neutrons:

A. Chietera, PhD thesis, University of Strasbourg, 2015
H.R. Bowman et al., Phys. Rev. 126 (1962) 2120 and Phys. Rev. 129 (1963) 2133
V.E. Bunakov, et al., Proc. “Interactions of Neutrons with Nuclei”, Dubna 2006, p293
A.M. Gagarski, et al., Proc. “Interactions of Neutrons with Nuclei”, Dubna 2012
N. Kornilov, Nucl. Phys. A 686, 187 (2001)
A.S. Vorobyev et al., Proc. “ISINN”, Dubna 2001, p276 and “ISINN”, Dubna 2009, p60
A. Mastsumoto, et al., J. Nucl. Sci. Technol. 49, 782 (2012)
C.B. Franklyn, et al., Phys. Lett. 78B (1978) 564

Some references on the ‘sudden Approximation’ model:

R.W. Fuller, Phys. Rev. 126, 648 (1962)
I. Halpern, Proc. “Physics and Chemistry of Fission” IAEA, Vienna, Vol. II, p369 (1965)
N. Carjan, et al., Phys. Rev. C82, 014617 (2010)
N. Carjan, et al., Phys. Rev. C85, 044601 (2012)
R. Capote, et al., Phys. Rev. C 93, 024609 (2016)

Some references on the Los Alamos model:

D.G. Madland, and J.R. Nix, Nucl. Sci. Eng. 81 (1982) 213
G. Vladuca and A. Tudora, Comput. Phys. Commun. 125 (1–3), 221–238 (2000)
F.-J. Hambsch, Annals of Nuclear Energy 32 (2005) 1032–1046
A. Tudora, Ann. Nucl. Energy 36 (2009) 72
D.G. Madland, and A.C. Kahler, Nucl. Phys. A957, 289 (2017)

References

Some references on recent Monte Carlo codes:

- **CGMF code**

S. Lemaire, et al., Phys. Rev. C 72, 024601 (2005)
S. Lemaire, et al., Phys. Rev. C 73, 014602 (2006)
P. Talou, et al., Phys. Rev. C 83, 064612 (2011)
B. Becker, et al., Phys. Rev. C 87, 014617 (2013)
P. Talou et al., Phys. Proc. 47, 39 (2013)
P. Talou, et al., Nucl. Data Sh. 118, 195–198 (2014)
I. Stetcu, et al., Phys. Rev. C 90, 024617 (2014)
P. Talou, et al., Phys. Rev. C **94**, 064613 (2016)

- **FIFRELIN code**

O. Litaize, O. Serot, Phys. Rev. C 82, 054616 (2010)
O. Litaize, et al., Eur. Phys. Journ. A 51 (2015) 177
O. Serot, et al., Phys. Proc. 59, 132 (2014)
D. Regnier, et al., Comput. Phys. Commun. 201, 19–28 (2016)

- **FREYA Code**

J. Randrup, R. Vogt, Phys. Rev. C 80, 024601 (2009)
R. Vogt and J. Randrup: Phys. Rev. C 80, 044611 (2009)
R. Vogt and J. Randrup: Phys. Rev. C 84, 044621 (2011)
R. Vogt, et al., Phys. Rev. C 85, 024608 (2012)
R. Vogt, J. Randrup, Nucl. Data Sheets 118, 220 (2014)
J.M. Verbeke et al., Com. Physics Comm. 191, 178 (2015)

- **GEF Code**

K.-H. Schmidt, B. Jurado, Phys. Rev. Lett. 104, 212501 (2010)
K.-H. Schmidt, B. Jurado, Phys. Rev. C 83, 061601 (2011)
K.-H. Schmidt et al., Nucl. Data Sheets 131, 107 (2016)

References

Some references on delayed neutrons:

L. Mathieu, et al., JINST 7 P08029 (2012)
T. Kawano, et al., Phys. Rev. C78, 054601 (2008)
T.K. Lane and E.J. Parma, SANDIA Report, SAND2015-7024 (2015)
NEA, WPEC-6 Report (2002)
JEFF Report 20, NEA-OECD (2009)

Some references on Theory of prompt particle emission and nuclear models

R. Capote et al., Nucl. Data Sheets 110, 3107 (2009).
T. Ericson and V. Strutinski, Nucl. Phys. 8, 284 (1958)
T. Ericson, Advances in Nuclear Physics **6**, 425 (1960)
H.-H. Knitter et al., in "The Nuclear Fission Process", C. Wagemans ed., CRC Press 1991
R. Vandenbosch and J.R. Huizenga : "Nuclear Fission" , Academic Press, 1973
H. Marten, A. Ruben, Sov. At. Ener. 69, 583 (1990).
A. Ruben and H. Marten and D. Seeliger, Z. Phys. A, Hadrons and Nuclei, 338, 67-74 (1991)
J. Terrell, Phys. Rev. 113, 527 (1959).
J. Terrell: Phys. Rev. 108, 783 (1957)
A. Gilbert, A.G.W. Cameron, Can. J. Phys. 43, 1446 (1965).
U. Brosa, S. Grossmann, A. Muller, Phys. Rep. 197, 167 (1990).
W. Hauser, H. Feshbach, Phys. Rev. 87, 366 (1952).
V.F. Weisskopf, Phys. Rev. 52, 295 (1937)
W.D. Myers, W.J. Swiatecki, Nucl. Phys. A 601, 141 (1996)

References

Some references on Experimental works: neutrons

J.W. Boldeman and M. G. Hines, Nucl. Sci. and Eng. 91,114 (1985)
H.R. Bowman et al., Phys. Rev. 126 (1962) 2120
H.R. Bowman et al., Phys. Rev. 129 (1963) 2133
C. Budtz-Jørgensen, H.H. Knitter, Nucl. Phys. A 490, 307 (1988)..
A. Gook et al., Phys. Rev. C 90, 064611 (2014)
F.-J. Hambsch, Nuclear Physics A 726 (2003) 248–264
F.-J. Hambsch et al., Nucl. Phys. A 491, 56 (1989).
F.-J. Hambsch, Annals of Nuclear Energy 32 (2005) 1032–1046
K. Nishio et al., Nucl. Phys. A 632, 540 (1998).
K. Nishio et al., Jour. of Nucl. Sc. and Techn., 35, 631 (1998)
N. Kornilov et al., Nucl. Sci. Eng. 165, 117 (2010)
N. Kornilov, in "Fission Neutrons", Ed. Springer, 2015 and references therein
H. Naik et al., Nucl. Phys. A 612, 143 (1997).
H. Naik et al., Phys. G: Nucl. Part. Phys. 30, 107 (2004).
W. Mannhart, Report IAEA-TECDOC-410 (1987) p. 158.
F. Pleasonton et al., Phys. Rev. C 6, 1023 (1972).
F. Pleasonton, Nucl. Phys. A 213, 413 (1973)
H. Nifenecker et al., Nucl. Phys. A 189, 285 (1972)
A.S. Vorobyev et al., EPJ Web of Conferences 8, 03004 (2010).
A.S. Vorobyev et al., Proc. "ISINN", Dubna 2001, p276
A.S. Vorobyev et al., Proc. "ISINN", Dubna 2009, p60
A.S. Vorobyev et al., Proc. Int. Conf. ND 2004, Santa Fe, USA, 2004, AIP Proceedings CP769, 613 (2005)
K. Skarsvag, Nucl. Phys. 253, 274 (1975)
T. Ohsawa, in IAEA Report INDC(NDS)-0541 (2009) p. 71.
Sh. Zeynalov et al., Proc. "Nuclear Fission and Fission-Product Spectroscopy", AIP Conf. Proc. 1175, p359 (2009)
Sh. Zeynalov et al., J. Korean Phys. Soc. **59**, 1396 (2011)
Y. Zhoa et al., Phys. Rev. C 62, 014612 (2000)
C. Signarbieux et al., Phys. Lett. 39B, 503 (1972)
H. W. Schmitt et al., Phys. Rev. 141, 1146 (1966)
P. Santi and M. Miller, Nucl. Sci. and Eng. 160, 190–199 (2008)
R. Müller et al., Phys. Rev. C 29, 885 (1984)
J. Fréhaut, in Proc. ND-1988, Mito Conf. 1988, IAEA 1989, p81
J. Fréhaut, IAEA report, INDC (NDS) -220, 1989, p 99
R. Gwin, Nucl. Sci. Eng 87,381 (1984)
R.L. Walsh et al., Nucl. Phys. A276 (1977) 189
Naqvi et al., Phys. Rev. C34, 218 (1986)

References

Some references on Experimental works: gamma

R. Billnert, F.-J. Hambsch, A. Oberstedt, S. Oberstedt, Phys. Rev. C 87, 024601 (2013).
A. Chyzh, C.Y. Wu, E. Kwan et al.: Phys. Rev. C85, 021601 (2012)
A. Chyzh, C. Y. Wu, E. Kwan et al: Phys. Rev. C 87, 034620 (2013)
A. Chyzh, C.Y. Wu, E. Kwan et al.: Phys. Rev. C 90,014602 (2014)
A. Gatera et al., Phys, Rev. C 95, 064609 (2017)
A. Oberstedt, T. Belgya et al: Phys. Rev. C 87, 051602(R) (2013)
A. Oberstedt, in EPJ web of Conference, (2017), to be published
S. Oberstedt, Eur. Phys. Journ. A 51, 178 (2015)
S. Oberstedt et al., Phys. Rev. C 93, 054603 (2016)
H. Nifenecker, C. Signarbieux, M. Ribrag et al: Nucl. Phys. A 189, 285 (1972)
O. Serot et al., JEC-doc 1828, NEA Report, 2017
P. Glassel, R. Schmid-Fabian, D. Schwalm, D. Habs, H.U.V. Helmolt, Nucl. Phys. A 502, 315c (1989).
C. Signarbieux et al.: Phys. Lett. 39B, 503 (1972)
V.V. Verbinski, H. Weber, R.E. Sund, Phys. Rev. C 7, 1173 (1973).
J.B. Wilhelmy, E. Cheifetz, J.R.C. Jared et al : Phys. Rev. C 5, 2041 (1972)

Commissariat à l'énergie atomique et aux énergies alternatives
Centre de Saclay | 91191 Gif-sur-Yvette Cedex
T. +33 (0)1 XX XX XX XX | F. +33 (0)1 XX XX XX XX

Direction
Département
Service